© 2014. Published by The Company of Biologists Ltd | Development (2014) 141, 1366-1380 doi:10.1242/dev.101352

RESEARCH ARTICLE

The *Drosophila* FHOD1-like formin Knittrig acts through Rok to promote stress fiber formation and directed macrophage migration during the cellular immune response

Uwe Lammel[1,*], Meike Bechtold[1,*], Benjamin Risse[2], Dimitri Berh[2], Astrid Fleige[1], Ingrid Bunse[1], Xiaoyi Jiang[2], Christian Klämbt[1] and Sven Bogdan[1,‡]

ABSTRACT

A tight spatiotemporal control of actin polymerization is important for many cellular processes that shape cells into a multicellular organism. The formation of unbranched F-actin is induced by several members of the formin family. *Drosophila* encodes six formin genes, representing six of the seven known mammalian subclasses. Knittrig, the *Drosophila* homolog of mammalian FHOD1, is specifically expressed in the developing central nervous system midline glia, the trachea, the wing and in macrophages. *knittrig* mutants exhibit mild tracheal defects but survive until late pupal stages and mainly die as pharate adult flies. *knittrig* mutant macrophages are smaller and show reduced cell spreading and cell migration in *in vivo* wounding experiments. Rescue experiments further demonstrate a cell-autonomous function of Knittrig in regulating actin dynamics and cell migration. Knittrig localizes at the rear of migrating macrophages *in vivo*, suggesting a cellular requirement of Knittrig in the retraction of the trailing edge. Supporting this notion, we found that Knittrig is a target of the Rho-dependent kinase Rok. Co-expression with Rok or expression of an activated form of Knittrig induces actin stress fibers in macrophages and in epithelial tissues. Thus, we propose a model in which Rok-induced phosphorylation of residues within the basic region mediates the activation of Knittrig in controlling macrophage migration.

KEY WORDS: F-actin, *Drosophila*, Formin, Stress fiber, Tracheal development, Macrophages, Cellular immune response

INTRODUCTION

The development of multicellular organisms crucially depends on the ability of cells to respond to extracellular cues and to reshape and migrate within the context of the forming tissue (Pollard and Borisy, 2003; Pollard and Cooper, 2009). These processes require the tightly controlled polymerization of actin filaments. Eukaryotic cells have evolved different actin-nucleating proteins promoting the rate-limiting nucleation reaction, i.e. the formation of stable multimers of actin monomers (Firat-Karalar and Welch, 2011). The ubiquitous Arp2/3 complex is one of the best-studied actin nucleators and initiates actin filament branches on sides of pre-existing filaments (Pollard and Borisy, 2003; Pollard and Cooper, 2009). Unlike Arp2/3, all other known actin nucleators produce unbranched filaments, including the formins or tandem-monomer-binding nucleators such as spire or JMY (Campellone and Welch, 2010; Carlier et al., 2011).

Formins assemble diverse cellular structures by nucleating unbranched actin filaments such as the cytokinetic contractile ring, stress fibers and filopodia (Goode and Eck, 2007). Defining features of all formins are formin homology domains 1 and 2 (FH1 and FH2). The homodimeric FH2 domain is thought to induce actin nucleation by stabilizing actin dimers, whereas the proline-rich FH1 domain promotes elongation by delivering profilin-bound actin monomers to the growing barbed filament end (Kovar, 2006). Most formins also contain additional conserved domains that regulate the activity, localization and interaction with regulatory binding partners. Mammals possess fifteen formins clustered into seven families based on domain similarities (Schönichen and Geyer, 2010). These families include the Diaphanous-related proteins (Dia), the Disheveled-associated activators of morphogenesis (Daam), the Formin-like proteins (FMNL), the Inverted formins (INF), the FH1/FH2 domain-containing proteins (FHOD/FHOS), the Delphin proteins and the group of FMN formins. Among all formins the Diaphanous-related formins (DRF) are best understood (Schönichen and Geyer, 2010). This group includes autoinhibited formins such as Dia, DAAM and FMNL, which are direct effectors of Rho GTPases (Goode and Eck, 2007). The autoinhibition of DRF is mediated by an intramolecular interaction between the C-terminal Diaphanous autoregulatory domain (DAD) and the N-terminal Diaphanous inhibitory domain (DID/FH3) (Otomo et al., 2005). Binding of Rho GTPases to the GTPase-binding domain (GBD) adjacent to the DID/FH3 domain results in the activation of the formin protein.

Members of the FHOD formin family share the characteristic FH1, FH2 and DAD domains with other DRFs, but their mode of activation is less well understood. Unlike DRF family members, mammalian FHOD1 binds Rac and Rho but not Cdc42 (Gasteier et al., 2003; Westendorf and Koka, 2004). Although activated Rac1 recruits FHOD1 to the membrane, Rac binding is not sufficient for its activation (Gasteier et al., 2003; Gasteier et al., 2005). Structural analyses further confirmed significant differences of the N-terminal GBD of FHOD1, suggesting a different role beyond autoregulation (Schulte et al., 2008). Previous studies revealed that phosphorylation of the C-terminal DAD might be an important regulatory modification for FHOD activation. Co-expression of FHOD1 and the Rho-associated kinase Rok results in a strong induction of stress fibers. A similar phenotype is observed upon expression of a constitutively active FHOD1 protein lacking the C-terminal DAD (Takeya and Sumimoto, 2003; Takeya et al., 2008). Remarkably, recent *in vitro* actin polymerization assays with recombinant FHOD1-ΔDAD protein revealed that FHOD1 may act as a combined actin capping and bundling factor rather than an actin

[1]Institute for Neurobiology, University of Münster, 48149 Münster, Germany.
[2]Institute for Computer Science, University of Münster, 48149 Münster, Germany.
*These authors contributed equally to this work

‡Author for correspondence (sbogdan@uni-muenster.de)

Received 17 July 2013; Accepted 19 January 2014

Development (2014) doi:10.1242/dev.101352

nucleator promoting actin polymerization (Schönichen et al., 2013). Indeed, constitutively active forms of FHOD1 inhibit actin assembly by capping growing actin filaments (Schönichen et al., 2013). Thus, the strong induction of stress fibers observed in cell transfection experiments might be the result of bundling pre-existing actin filaments.

The *in vivo* functions of the FHOD-related proteins in a multicellular context are less well studied. The muscle-specific FHOD3 has been implicated in myogenesis. *Fhod3* mutant mice display strong defects in myofibril maturation resulting in embryonic lethality (Iskratsch et al., 2010; Kan-O et al., 2012a; Kan-O et al., 2012b; Taniguchi et al., 2009). This muscle-specific function of FHOD isoforms seems to be evolutionarily conserved and *C. elegans* lacking the *Fhod*3-related gene shows prominent cytoskeletal organization defects in muscle cells (Mi-Mi et al., 2012). The developmental functions as well as the formin activity of *Drosophila* FHOD have not been addressed. However, recent microarray analyses revealed that the only member of the FHOD family in *Drosophila* becomes highly upregulated upon bacterial infection and in autophagic programmed cell death during pupal metamorphosis (Anhezini et al., 2012; Johansson et al., 2005).

Here, we present the functional analysis of *knittrig*, which encodes the *Drosophila* FHOD protein. During embryonic development *knittrig* is expressed in midline glia, subsets of tracheal cells and in macrophages. In larval stages, *knittrig* is expressed in the developing imaginal discs, including eye and wing imaginal discs. Mutant embryos show mild tracheal defects but can survive until adulthood and they show a characteristic wrinkled wing phenotype. Rescue experiments indicate a cell-autonomous function of *knittrig* in macrophage spreading and migration. Live cell imaging and additional gain-of-function experiments further suggests a model in which the Rho-dependent kinase Rok activates Knittrig to promote actin stress fiber formation mediating the trailing edge retraction of migrating macrophages.

RESULTS

Knittrig represents the *Drosophila* FHOD formin subclass

The *Drosophila* genome encodes six of the seven known mammalian formin families (Liu et al., 2010; Schönichen and Geyer, 2010). Loss-of-function analyses of *diaphanous* (*dia*), *cappuccino* (*capu*), *disheveled associated activator of morphogenesis* (*daam*) and *formin 3* (*form3*, *CG33556*) have previously been reported, representing the Dia, FMN, DAAM and INF family of formins, respectively (Castrillon and Wasserman, 1994; Emmons et al., 1995; Matusek et al., 2006; Tanaka et al., 2004). *CG32030* encodes a member of the FHOD protein family (Fhos). Based on the wing phenotype of mutant adult flies (see below) the gene *CG32030* was termed *knittrig* (German for wrinkled). *knittrig* (*knit*) encodes up to nine predicted isoforms that differ mostly in their C-terminal sequences (Fig. 1A,B; FlyBase). The largest isoform, Knittrig^{PI}, contains an additional large N-terminal exon encoding ~1000 amino acids without any sequence similarity to other known proteins, whereas the shortest isoform Knittrig^{PB} lacks C-terminal exons encoding the DAD (Fig. 1B). Isoform Knittrig^{PA} shows high homology to mammalian FHOD1 protein (Fig. 1B,C). It contains well-conserved FH2 and FH1 domains followed by a C-terminal DAD. In addition, it harbors regulatory FH3 and GBD domains at the N-terminus. Unlike mammalian FHOD1, the DAD of Knittrig only contains one DAD core motif followed by a conserved cluster of positively charged residues (Fig. 1E). The remaining five isoforms show variations in exons encoding either the C-terminal DAD (Knittrig^{PB}) or the N-terminal GBD (Knittrig^{PF}).

Identification of *knittrig* mutants

We first generated *knittrig* mutants by imprecise excision utilizing the *AA142* enhancer trap insertion P(lwB)^{AA142} (Klämbt et al., 1991). The breakpoints of two deletions Δ*140* and Δ*1* were determined (Fig. 1A). Additionally, we generated one EMS-induced mutant allele (*knittrig*^{EMS}). The deletion Δ*1* completely removes sequences encoding the *knittrig* isoforms PA, PB, PD, PE, PF and PG (deletion spans from 8,762,007 to 8,818,577) and a cluster of small genes mostly encoding predicted chitin-binding proteins. The Δ*140* deletion lacks the 5′ exons of isoforms PI, PJ and PH as well as the first exon of all mRNA encoding isoforms and parts of the *Paramyosin* (*Prm*) (Liu et al., 2003) gene (deletion spans from 8,736,935 to 8,762,911).

The *knittrig*$^{\Delta 1}$ deletion results in reduced viability and only rare escaper flies are found in homozygosity or in trans to large deficiencies. Likewise, rare escaper flies are found in trans to *knittrig*$^{\Delta 140}$, demonstrating that this phenotype is due to a specific loss of *knittrig* (Fig. 2A). The vast majority of mutants die during pupal stages or as pharate adult flies incapable of enclosing from the pupal case. Most of the escaper flies are unable to undergo complete wing inflation, causing characteristic wrinkled wings (Fig. 2B,C). Based on this phenotype the gene locus was termed *knittrig*. Some of the escaper flies show partially inflated and abnormally opaque wings, suggesting that the resorption of the wing epithelium or tracheal air-filling is incomplete (Fig. 2B). In agreement with this, mutant pupal wings appear normal (supplementary material Movie 1).

The *knittrig* gene is not uncovered by the deficiencies *Df(3L)BSC816* and *Df(3L)ED4416* (Fig. 1A, Fig. 2A). By contrast, *knittrig*$^{\Delta 1}$ and *knittrig*$^{\Delta 140}$ fail to complement the deficiencies *Df(3L)hi22*, *Df(3L)ScfR6*, *Df(3L)ED4421* or *Df(3L)ED4413*. *Prm*^{1} complements *knittrig*$^{\Delta 1}$ but not *knittrig*$^{\Delta 140}$. Importantly, re-expression of Knittrig (PA isoform, single copy) using the ubiquitous *arm*-Gal4 driver completely rescues both lethality and the wing phenotype of homozygous *knittrig*$^{\Delta 1}$ flies. Thus, both lethality and the wing phenotype result from a loss of Knittrig function and are not due to a loss of predicted chitin-binding proteins, which are also removed in *knittrig*$^{\Delta 1}$ mutants.

Expression of *knittrig* during development

To gain insight into the developmental functions of Knittrig we examined the temporal and spatial expression of *knittrig* by *in situ* hybridization (Fig. 3). *knittrig* expression can first be detected in early stage 12 embryos in the salivary gland placodes and midline glial progenitor cells (Fig. 3A,B). To study *knittrig* expression we also followed β-galactosidase expression directed by the *AA142* enhancer trap element, which closely resembles the transcription pattern of the *knittrig* gene (Fig. 3). Note that expression of the *AA142* enhancer trap marker is confined to nuclei due to expression of β-galactosidase with a nuclear import signal. Expression in the CNS midline glia persists throughout embryonic and larval development (Fig. 3E,F). In stage 16 embryos, *knittrig* RNA expression is also found in a ring of cells around the anal plates (Fig. 3G,H) and in hemocytes (Fig. 3F,G, arrows). In addition, *knittrig* is expressed in the tracheal system and the dorsal vessel (Fig. 3E,F; data not shown). Double-labeling experiments indicate that *knittrig* is expressed in the so-called tip cells that advance the tracheal tree towards the CNS (Fig. 3L′, arrows). Later on in larval development, *knittrig* is expressed in the CNS midline glia and in several imaginal discs. In third instar wing imaginal discs *knittrig* expression is found in cells of the presumptive wing margin (Fig. 3I). In the eye imaginal discs, *knittrig* is expressed at the morphogenetic furrow (Fig. 3J).

Development (2014) doi:10.1242/dev.101352

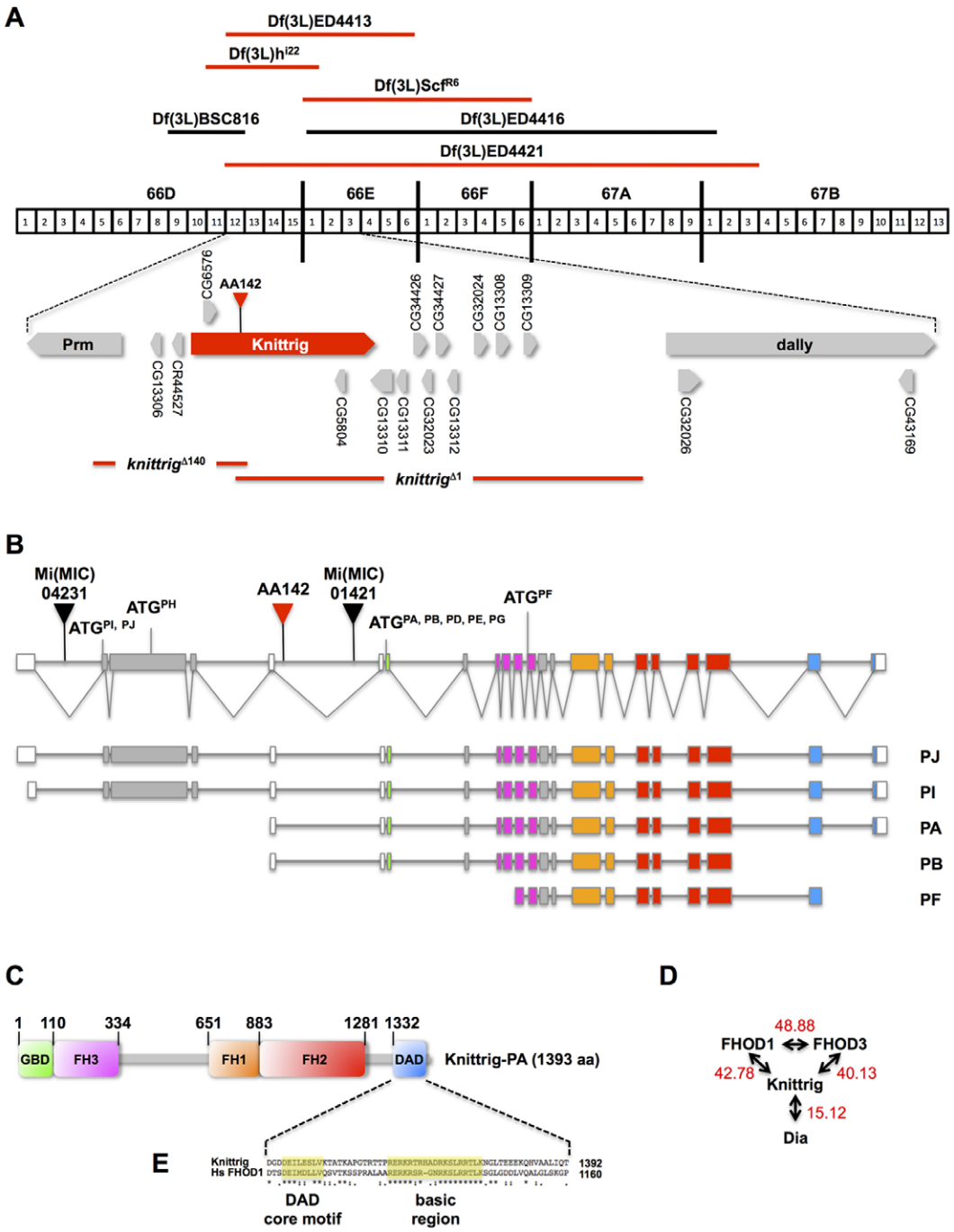

Fig. 1. Knittrig represents the *Drosophila* FHOD formin subclass. (A) Schematic overview of the *knittrig* gene locus. *knittrig* is located on the third chromosome in the cytological region 66D12-E2. The deficiency chromosomes *Df(3L)hi22*, *Df(3L)ScfR6*, *Df(3L)ED4421* and *Df(3L)ED4413* (red) remove *knittrig* function. The *knittrig* gene locus is not uncovered by the deficiency *Df(3L)BSC816* or *Df(3L)ED4416* (black). The *AA142* enhancer trap insertion P(lwB)^{AA142} is indicated by the red triangle. The breakpoints of the *knittrig* deletions Δ1 and Δ140 are indicated. The deletion in *knittrig*$^{\Delta 1}$ starts at the insertion point of *AA142* and ends in front of the *dally* locus, whereas the deletion in *knittrig*$^{\Delta 140}$ starts 2 kb downstream from the insertion point of P(lwB)^{AA142} and spans to intron 4 of *Paramyosin* (*Prm*). (B) Schematic view of the various *knittrig* isoforms. The *AA142* enhancer trap insertions P(lwB)^{AA142} (red triangle) and two additional Mi(MIC)-P element insertions (black triangle) are indicated. Differential splicing leads to the two largest Knittrig protein isoforms PJ/I and PA. The exons of the *knittrig* isoform PA are colored according to the encoding domains: green, GBD; purple, FH3; gray, non-conserved region; orange, FH1; red, FH2; blue, DAD. (C) Schematic view of the full-length Knittrig-PA protein. (D) Comparative sequence analysis between Knittrig, *Drosophila* Dia and human FHOD1 and FHOD3 proteins. The numbers refer to the ClustalW sequence alignment score (Thompson et al., 1994). Knittrig shows the highest degree of homology with human FHOD1. (E) ClustalW sequence alignment of the DADs from Knittrig-PA and human FHOD1 is shown. The conserved DAD core motif and the subsequent cluster of positively charged residues are highlighted in yellow. Identical residues are marked by an asterisk.

Loss of *knittrig* function affects tracheal morphogenesis

Since *knittrig* shows prominent expression in the tracheal system, we examined *knittrig* mutant embryos for possible tracheal defects during development. In wild type, trachea development starts at embryonic stage 11 when epidermal cells invaginate. The resulting tracheal sacs extend branches in a stereotypic manner and finally

Development (2014) doi:10.1242/dev.101352

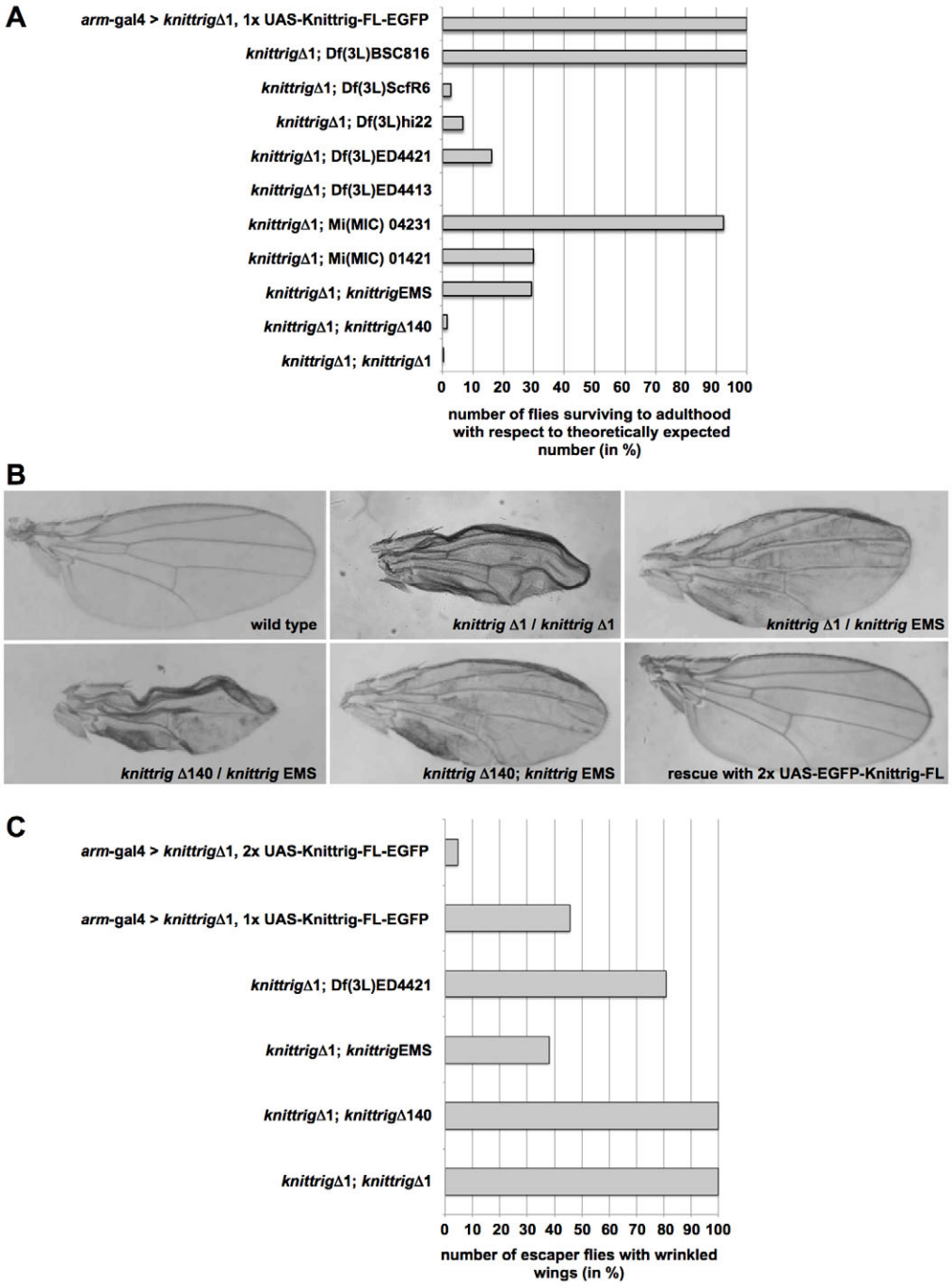

Fig. 2. Loss of Knittrig function affects viability and escaper flies show wrinkled wings.
(A) Complementation analysis of *knittrig* alleles. The percentage of adult flies with respect to the number of expected animals was calculated (*n*=300-1000 flies were counted in total for each genotype). Homozygous or transheterozygous allele combinations such as $knittrig^{\Delta 1}$/$knittrig^{\Delta 1}$, $knittrig^{\Delta 1}$/$knittrig^{\Delta 140}$ or $knittrig^{\Delta 1}$/*Df(3L)ED4413* result in rare escapers (0.1-1%). Note that the re-expression of a full-length Knittrig transgene driven by *arm*-Gal4 completely rescues lethality.
(B) Female adult wings of the indicated genotypes are shown. *knittrig* escaper flies show a prominent wrinkled wing phenotype. Some escaper flies exhibit partially inflated but abnormal, opaque wings.
(C) Quantification of the wrinkled wing phenotype. The percentage of escaper flies with wing defects was calculated (*n*=500-1000 flies in total were counted for each genotype). Note that the re-expression of two copies of full-length Knittrig transgene driven by *arm*-Gal4 substantially rescues the wing defects.

fuse to form an interconnected network of tracheal tubes by the end of embryogenesis (supplementary material Fig. S1A,C). In all *knittrig* mutant combinations, we observed a penetrant phenotype with reduced formation of ganglionic tracheal branches (supplementary material Fig. S1B,D). In wild type, these tracheae segmentally follow the peripheral nerves into the ventral nerve cord towards the ventral midline (Englund et al., 1999). In *knittrig* mutants, the majority of the embryos show disruption in at least one ganglionic branch (supplementary material Fig. S1B,D, arrows). Since the ganglionic tracheal branches supply oxygen to the ventral nerve cord, this might explain the 'leaky' lethality and the occurrence of a few eclosing homozygous *knittrig* flies. No abnormal phenotype was detected for the midline glial cells (data not shown).

knittrig function is required for macrophage cell spreading

The expression of *knittrig* in hemocytes suggests a possible function during the cellular immune response. Supporting this notion, *knittrig* expression is strongly upregulated in immune-challenged *Drosophila* hemocytes (Johansson et al., 2005; Valanne et al., 2007). To further analyze *knittrig* function in hemocytes we examined macrophages, which constitute the most abundant cell type in the hemolymph (Wood and Jacinto, 2007). We isolated macrophages from wild-type and homozygous $knittrig^{\Delta 1}$ mutant larvae and prepupae. To visualize the actin cytoskeleton at high spatial resolution we applied structured-illumination microscopy to fixed cells stained with fluorescently labeled phalloidin (Fig. 4). Wild-type macrophages show a broad lamellipodial actin filament network at the cell front and actin stress fiber-like structures at the

Development (2014) doi:10.1242/dev.101352

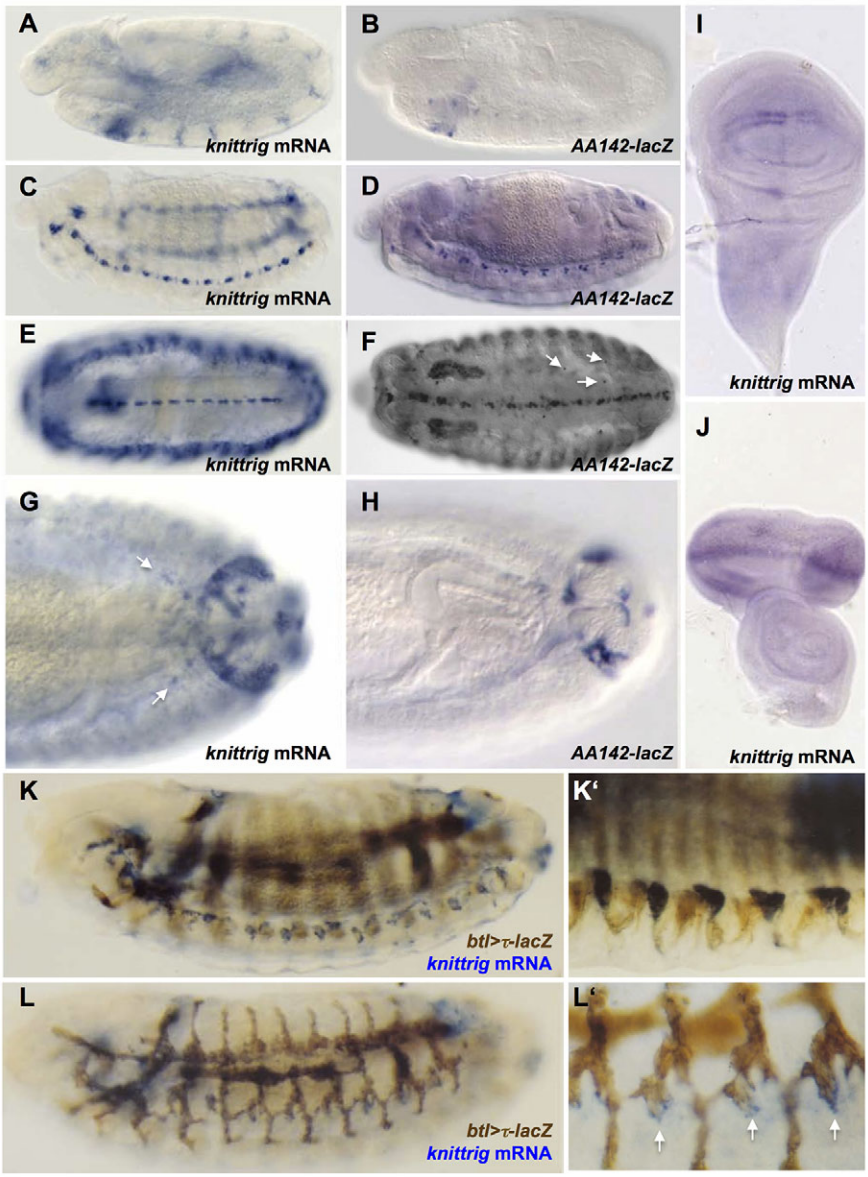

Fig. 3. Knittrig is expressed in midline glia, tracheal cells and hemocytes. *In situ* hybridization of *knittrig* mRNA (A,C,E,G,I,J) and the enhancer trap-driven expression of *lacZ* visualized by immunohistochemistry (β-galactosidase) in embryonic stages (B,D,F) are shown. The expression pattern for *knittrig* mRNA expression is similar in the enhancer trap and in *in situ* hybridization. The embryonic expression starts at early stage 12 in the midline glia cells and the salivary gland placodes (A,B). At stage 13, expression in the midline glia persists and the forming tracheae show additional *knittrig* expression (C,D). The midline glia are still marked in later stages. (E,F) The lateral body regions in late stage embryos become more strongly labeled by *in situ* hybridization, and single scattered cells (hemocytes) located in the hemocoel are marked (arrows). (G,H) Strong expression is also found in a ring of cells around the anal plates (arrows). (I,J) In third stage larval imaginal discs, expression is found in the region anterior to and within the morphogenetic furrow of the eye imaginal discs. In the wing imaginal discs, elevated levels of *knittrig* are found in the region flanking the presumptive wing margin. (K-L′). *In situ* hybridization/peroxidase immunohistochemistry double labeling confirmed the expression of *knittrig* in tip cells of tracheal branches (arrows).

back around the nucleus (Fig. 4A) (Sander et al., 2013). Cell spreading is increased on cover glasses coated with the lectin concavalin A (ConA). We further differentiate between lectin-mediated cell spreading and integrin-mediated cell spreading on uncoated surfaces, as shown recently (Jani and Schöck, 2007; Kadandale et al., 2010). Loss of *knittrig* function does not affect lamellipodia formation, in contrast to what has been reported previously for downregulation of the WAVE-Arp2/3 pathway in hemocyte-like S2R+ cells or macrophages (Bogdan and Klämbt, 2003; Kunda et al., 2003; Zobel and Bogdan, 2013; Sander et al., 2013). However, we found that *knittrig* mutant macrophages display strong defects in cell flattening and spreading on both ConA-coated and uncoated surfaces (Fig. 4B,E). Consistently, hemocyte-specific RNAi-mediated knockdown of *knittrig* using the *hml*Δ-Gal4 driver results in similar cell spreading defects, indicating a cell-autonomous requirement of Knittrig in cell spreading (Fig. 4E) (Sinenko and Mathey-Prevot, 2004). Supporting this notion, hemocyte-specific re-expression of a full-length Knittrig protein in *knittrig*$^{\Delta 1}$ mutant cells substantially rescues the cell spreading defects (Fig. 4C,E).

Knittrig localizes at the rear of migrating macrophages *in vivo*

To further investigate the cellular requirement of Knittrig we analyzed its subcellular localization in macrophages. Since our antibodies failed to detect the endogenous protein, we generated an EGFP-tagged Knittrig transgene using the ΦC31 integrase system (Bischof et al., 2007). We expressed the EGFP-Knittrig-FL (isoform PA) transgene in larval and pupal macrophages using the *hml*Δ-Gal4 driver.

Spinning disc confocal imaging confirmed highly dynamic membrane protrusions of isolated transgenic macrophages *ex vivo*, as shown recently (Sander et al., 2013). EGFP-Knittrig localizes throughout the cytoplasm with nonspecific cytoplasmic filling extending into membrane ruffles (Fig. 4F; supplementary material Movie 2). Moreover, dynamic vesicular structures in the perinuclear region were often marked by EGFP-Knittrig (Fig. 4F; supplementary material Movie 2).

Since isolated macrophages become adherent shortly after cell plating, resulting in a non-motile cell behavior similar to S2 culture cells (Sander et al., 2013), we next analyzed the localization of

Development (2014) doi:10.1242/dev.101352

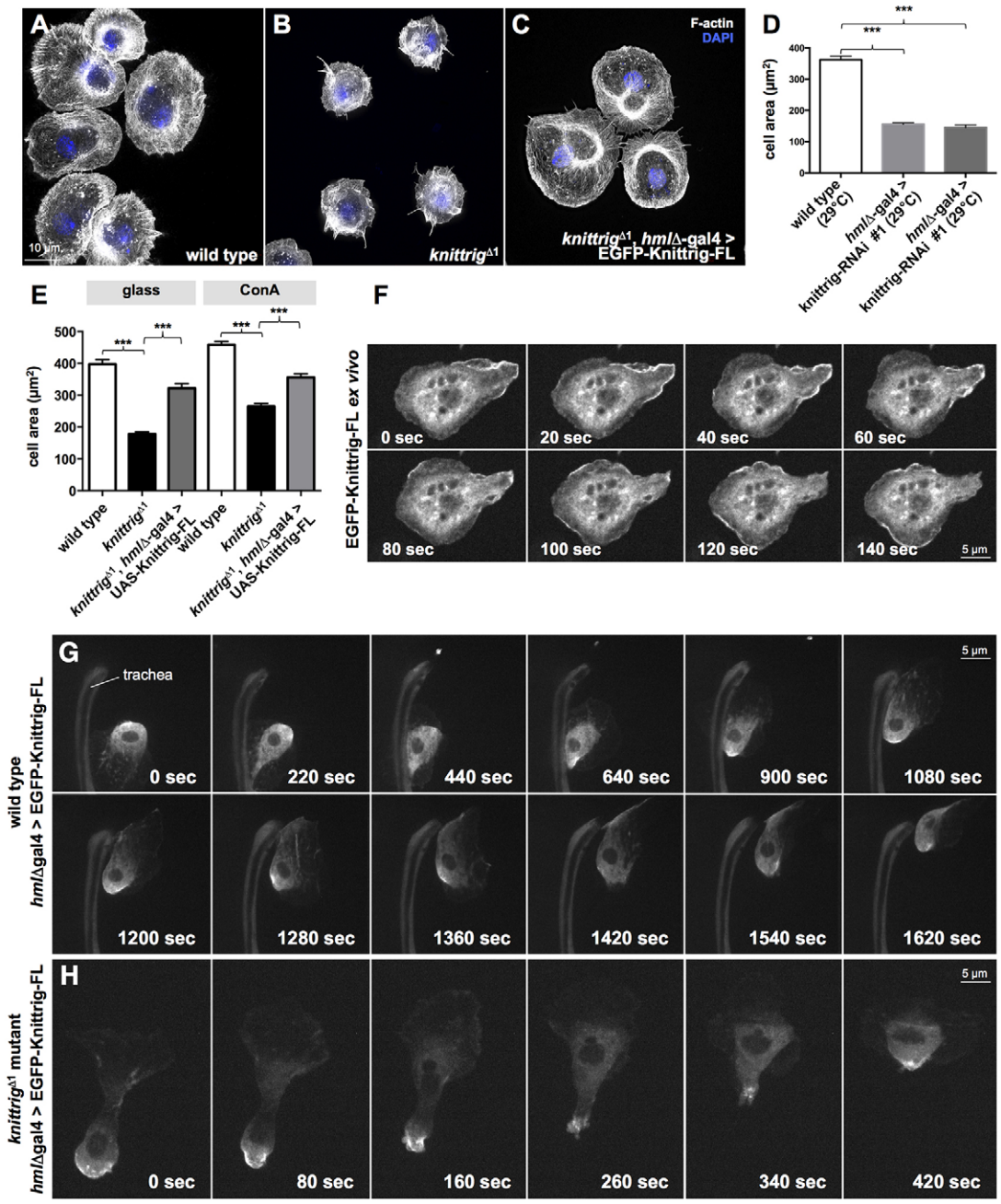

Fig. 4. *knittrig* regulates macrophage cell spreading. (A-C) Structured illumination microscopy (SIM) images of *Drosophila* larval (A) wild-type, (B) homozygous *knittrig*$^{\Delta 1}$ and (C) homozygous *knittrig*$^{\Delta 1}$ macrophages re-expressing full-length Knittrig driven by the *hml*Δ-Gal4 driver, stained with phalloidin (white, F-actin) and DAPI (blue, nuclei). (D) Quantification of cell spread area of wild-type, mutant and rescued macrophages plated on ConA-coated coverslips. (E) Macrophage-specific knockdown of *knittrig* using the *hml*Δ-Gal4 driver results in similar cell spreading defects. Error bars represent s.e.m. ***P<0.0001. (F) Series of time-lapse images of an isolated macrophage expressing EGFP-Knittrig-FL. See also supplementary material Movie 2. (G,H) Series of time-lapse images of migrating macrophages expressing EGFP-Knittrig-FL taken from (G) wild-type and (H) homozygous *knittrig*$^{\Delta 1}$ mutant prepupae (2-4 hours APF). See also supplementary material Movies 3, 4a,b.

Knittrig in migrating wild-type and *knittrig*$^{\Delta 1}$ mutant macrophages *in vivo*. The EGFP-Knittrig-FL transgene was expressed only weakly to allow live cell imaging on dorsal subepidermal macrophages of 2- to 4-hour pupae (Moreira et al., 2013). At this stage, wild-type macrophages are morphologically highly polarized with broad lamellipodial protrusions and migrate randomly beneath the epidermis or along tracheae (Moreira et al., 2013) (Fig. 4G). Knittrig accumulates at the rear of these highly polarized macrophages in a dynamic fashion (Fig. 4G; supplementary material Movie 3). Next, we examined the localization of the EGFP transgene in homozygous *knittrig*$^{\Delta 1}$ mutant macrophages lacking the endogenous protein (Fig. 1). This expression regime efficiently rescued the macrophage spreading and cell migration phenotype (see below). In addition, Knittrig localizes strongly to the retracting uropod-like structures of migrating mutant macrophages (Fig. 4G; supplementary material Movies 4a,b). These cells often show an extensive blebbing activity at the cell rear, which is thought to be controlled by the coordinated action of Rho/Rok-mediated

Development (2014) doi:10.1242/dev.101352

actomyosin contractions (Fig. 4G; supplementary material Movie 4a) (Sánchez-Madrid and Serrador, 2009).

knittrig function is required for macrophage migration

Cell spreading defects related to the phenotypes mentioned above were recently observed in macrophages deficient for *Drosophila Rho1* (Kadandale et al., 2010). Additionally, *Rho1* mutant macrophages are impaired in their recruitment to epidermal wounds (Kadandale et al., 2010). Given the distinct localization of Knittrig to the cell rear we examined a possible role in directed cell migration and analyzed the migratory behavior of macrophages *in vivo* upon laser-induced wounding in pupal wings. Wild-type macrophages immediately migrate towards a laser-induced wound or single ablated cell (Fig. 5A; supplementary material Movie 5). To quantify this migratory behavior, a local histogram-based image analysis technique was developed to calculate an overall migration score (Fig. 5C-E). This score, called the histogram-based macrophage migration score (HMMS), measures the number of foreground pixels (i.e. macrophages) around the stimulus (wound) over time. High HMMS values indicate that most detected cells (relative to the overall cell density) are located around the wound, whereas small values (close to 0) indicate a sparse macrophage density around the wound. Furthermore, the slope of the score serves as an indirect measure of the migration speed, since a strong gradient is caused by a rapid increase of foreground pixels between consecutive frames (Fig. 5C,D). The median HMMS, plotted for wild-type, mutant and RNAi measurements over time clearly show that cells deficient for *knittrig* are still able to respond and migrate to wound sites but the speed as well as the direction of migration are clearly impaired (Fig. 5F; supplementary material Movies 5, 6, 8-10). The differences in directed migration between wild-type and mutant or RNAi depleted macrophages are most obvious between 200 and 800 seconds after wounding, when a rapid increase can be measured in wild-type cells compared with mutant and RNAi

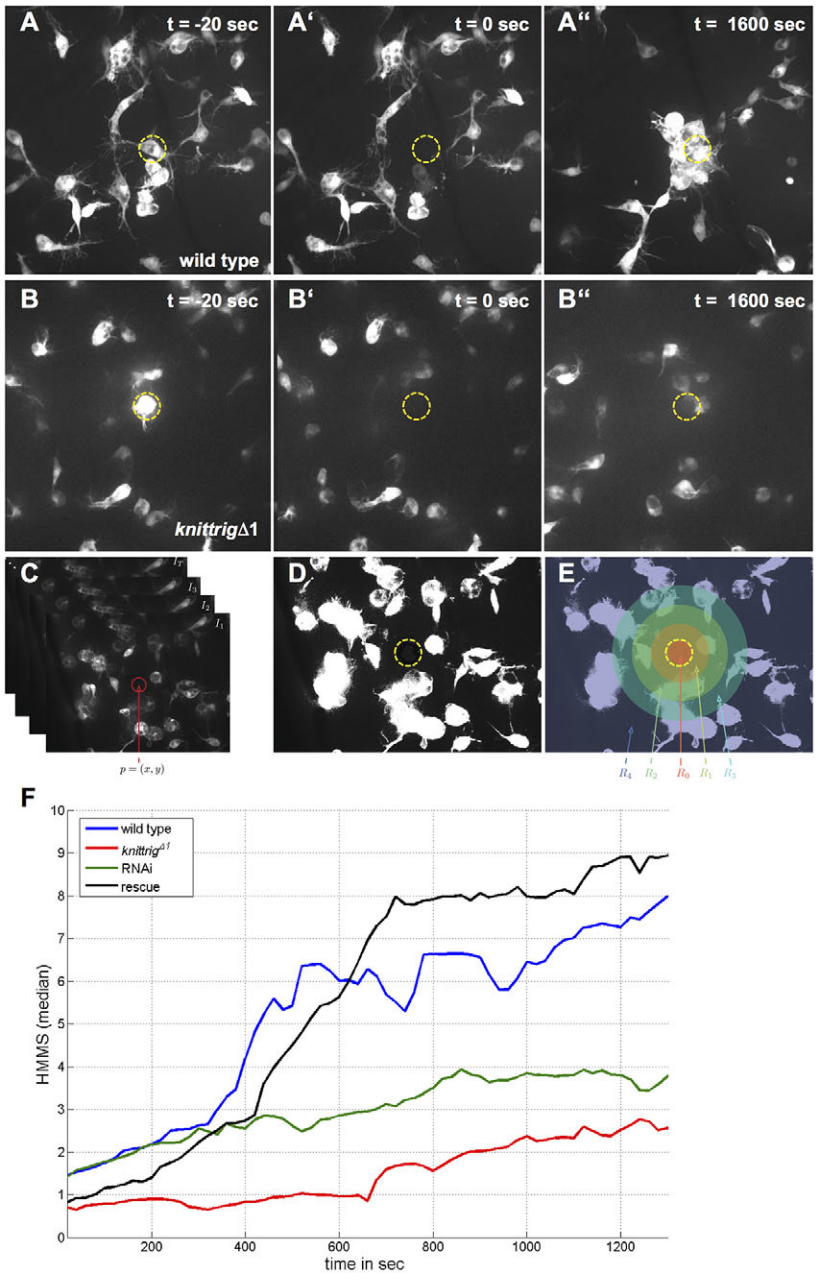

Fig. 5. Knittrig regulates macrophage cell migration during the immune response. (A-B″) Frames of spinning disc microscopy videos of migrating wild-type (A-A″) and *knittrig* mutant (B-B″) macrophages at the indicated time points, visualized by the expression of cytoplasmic EGFP. (C) Sketch of an exemplary unprocessed image stack I_1, ..., I_T as well as the wound position $p=(x, y)$. (D) Segmented image after applying thresholding procedure. White pixels are accounted as macrophage pixels. (E) Illustration of the local histogram regions. Concentric regions R_0, ..., R_3 around the stimulus and R_4 are highlighted. (F) Median HMMS values for wild-type (blue, n=10), *knittrig* RNAi (green, n=14), *knittrig*$^{\Delta 1}$ mutant (red, n=11) and rescued *knittrig*$^{\Delta 1}$ mutant (black, n=15) macrophage movies plotted for 1300 seconds after wounding. An overall higher median HMMS value is observed for the wild-type cells compared with *knittrig* RNAi and *knittrig* mutant cells, indicating more and faster movement towards the wound over time. See also supplementary material Movies 5-11.

Development (2014) doi:10.1242/dev.101352

depleted macrophages (Fig. 5F). Re-expression of Knittrig in homozygous *knittrig*$^{\Delta 1}$ mutant macrophages restores the migration defects (Fig. 5F; supplementary material Movie 7). Remarkably, rescued cells even show an increased migration speed, resulting in higher HMMS values compared with wild-type macrophages (Fig. 5F; supplementary material Movie 11). Thus, we conclude that *knittrig* is important for directed macrophage migration during the cellular wound response.

Knittrig promotes stress fiber formation in *Drosophila* S2 cells

As shown previously for mammalian FHOD1, we could demonstrate an interaction of Knittrig with Rho GTPases such as Rac1 and RhoA (but not Cdc42), but in a guanine-nucleotide independent manner (Fig. 6A) (Westendorf, 2001). Thus, binding to Rho GTPases does not seem to be a sufficient regulatory mechanism for the activation of Knittrig.

Deletion of the C-terminal inhibitory DAD results in activation of mammalian FHOD1 (Takeya and Sumimoto, 2003). The induction of actin stress fibers is the most prominent phenotype evoked by constitutively active FHOD1-ΔDAD in mammalian cell culture (Takeya and Sumimoto, 2003). To test the role of the DAD of Knittrig we performed gain-of-function analyses to examine the ability of Knittrig in regulating actin cytoskeleton organization. We generated N-terminally EGFP-tagged fusions of mutant Knittrig proteins containing distinct deletions in functional domains (Fig. 6B). Expression of a full-length Knittrig protein or the FH2 domain alone did not affect the overall actin cytoskeleton architecture in transfected *Drosophila* S2R+ cells (Fig. 6C; supplementary material Movie 12). Both proteins mainly distribute throughout the cytoplasm or accumulate in large cytoplasmic clumps (Fig. 6C). However, truncations of the conserved C-terminal basic cluster (ΔB) or of the complete DAD (ΔDAD) result in a strong reorganization of the actin cytoskeleton of transfected cells (Fig. 6C). The expression of either truncated protein induces the formation of thick actin bundles (Fig. 6C). Such unbranched actin bundles are never observed in wild-type S2R+ cells.

The highly conserved C-terminal cluster of positively charged residues in the Knittrig protein appears sufficient to mediate the autoinhibition, although cells expressing the ΔDAD truncation exhibit stress fiber-like structures more frequently. Since it is known that rigid surfaces further increase the mechanical forces promoting stress fiber formation (Burridge and Wittchen, 2013), we plated transfected cells on uncoated glass coverslips. Under these conditions, S2R+ cells expressing Knittrig-ΔDAD strongly induce large stress fibers reminiscent of Rho-induced stress fibers in mammalian fibroblasts (Fig. 6C). Live imaging analysis revealed a dynamic turnover of activated Knittrig in stress fibers (supplementary material Movies 13a,b).

To further examine Knittrig protein dynamics we performed FRAP experiments with cells expressing EGFP-Knittrig-ΔDAD plated on glass coverslips (Fig. 6D). We observed a rapid homogeneous recovery of EGFP-Knittrig-ΔDAD along stress fibers with half-life times ($t_{1/2}$) between 6 and 9 seconds and ~60-70% of the fluorescence recovered by 90 seconds (Fig. 6D,E). The turnover rates at the tips of stress fibers ($t_{1/2}$=6.74 seconds), where actin filaments are anchored to focal adhesions, seem to be substantially faster than at central regions within stress fibers ($t_{1/2}$=9.02 seconds), as shown recently for dorsal stress fiber formation in mammalian cell culture (Fig. 6D,E; supplementary material Movie 14) (Hotulainen and Lappalainen, 2006). These data indicate that active Knittrig constantly associates and dissociates with stress fibers.

Knittrig can be activated by Rok to promote stress fiber formation

Previous studies have demonstrated that phosphorylation of the C-terminal DAD by the Rho-dependent kinase Rok/Rock is an important regulatory modification for mammalian FHOD1 activation. The phosphorylated serine/threonine residues within the DAD are conserved between FHOD1 and Knittrig, suggesting that Knittrig might also be activated by Rok. We found that Knittrig can indeed be phosphorylated (Fig. 7A). Co-expression of EGFP-Knittrig-FL and an HA-tagged Rok in S2R+ cells results in increased serine phosphorylation of Knittrig (Fig. 7A). We next analyzed whether Rok is able to promote Knittrig-dependent actin stress fiber formation in S2R+ cells. Co-expression of full-length Rok (Rok-WT) and EGFP-Knittrig-FL indeed strongly induces stress fiber formation, whereas expression of Rok-WT or EGFP-Knittrig-FL alone has no effect on actin cytoskeleton organization (Fig. 7B, Fig. 6C). In contrast to wild-type Rok, a constitutively active variant (Rok-CAT 1-553aa) (Simões et al., 2010) already slightly induces actin stress fibers (Fig. 7C). Upon co-transfection of Rok-CAT and EGFP-Knittrig-FL stress fiber formation is strongly enhanced, even in cells plated on ConA (Fig. 7D,E). More importantly, these cells show dramatic cell contractions and dynamic membrane blebbing (supplementary material Movie 15). Remarkably, in those cells co-expressing Rok-CAT and EGFP-Knittrig-FL, Knittrig becomes entirely recruited to a ring-like structure in the cell center near the centrosome (supplementary material Movie 15). Additional live imaging analysis revealed a relocalization of Knittrig induced by Rok to regions of the microtubule organizing center (MTOC), where activated Rok has been found previously (supplementary material Movie 16) (Chevrier et al., 2002). In agreement with this observation, we frequently found cytokinesis defects upon Rok and EGFP-Knittrig-FL co-expression resulting in multinucleated cells (data not shown; Fig. 7H).

The functional interaction between Knittrig and Rho kinase in regulating stress fiber formation could also be observed *in vivo* in macrophages. Since early larval expression of active Knittrig or Rok gain-of-function inhibits the release of mature macrophages from the hematopoietic lymph gland into the hemolymph (data not shown), we used the Gal4/Gal80ts system to restrict expression to late third instar larvae (McGuire et al., 2003). Constitutively active Knittrig protein (ΔDAD) accumulates in actin stress fiber-like structures at the rear of isolated macrophages (Fig. 7F). Moreover, cells expressing elevated Knittrig-ΔDAD levels show an increased number of F-actin bundles, suggesting that Knittrig promotes the formation of these stress fiber-like structures in macrophages (Fig. 7F). Similar to observations in S2R+ cells, the co-expression of inactive full-length Knittrig with full-length Rok (Rok-WT) strongly induces stress fibers in macrophages (Fig. 7H). Again, expression of constitutively active Rok alone already induces stress fibers (Fig. 7I). Similarly, co-expression of Rok-CAT and Knittrig completely reorganizes actin filament bundles into a star-like pattern emerging from the cell center – a typical structure induced by Rok activation (Fig. 7J) (Leung et al., 1996).

Knittrig is able to remodel epithelial architecture *in vivo*

Finally, we examined whether active Knittrig also affects the organization of actin filaments in a multicellular context. Since ubiquitous expression of Knittrig-ΔDAD and Knittrig-ΔB results in early embryonic lethality we used the *patched* (*ptc*)-Gal4 driver to restrict expression. Overexpression of full-length Knittrig in wing imaginal discs did not affect the overall epithelial integrity or the level of F-actin. By contrast, expression of Knittrig-ΔB or Knittrig-

Development (2014) doi:10.1242/dev.101352

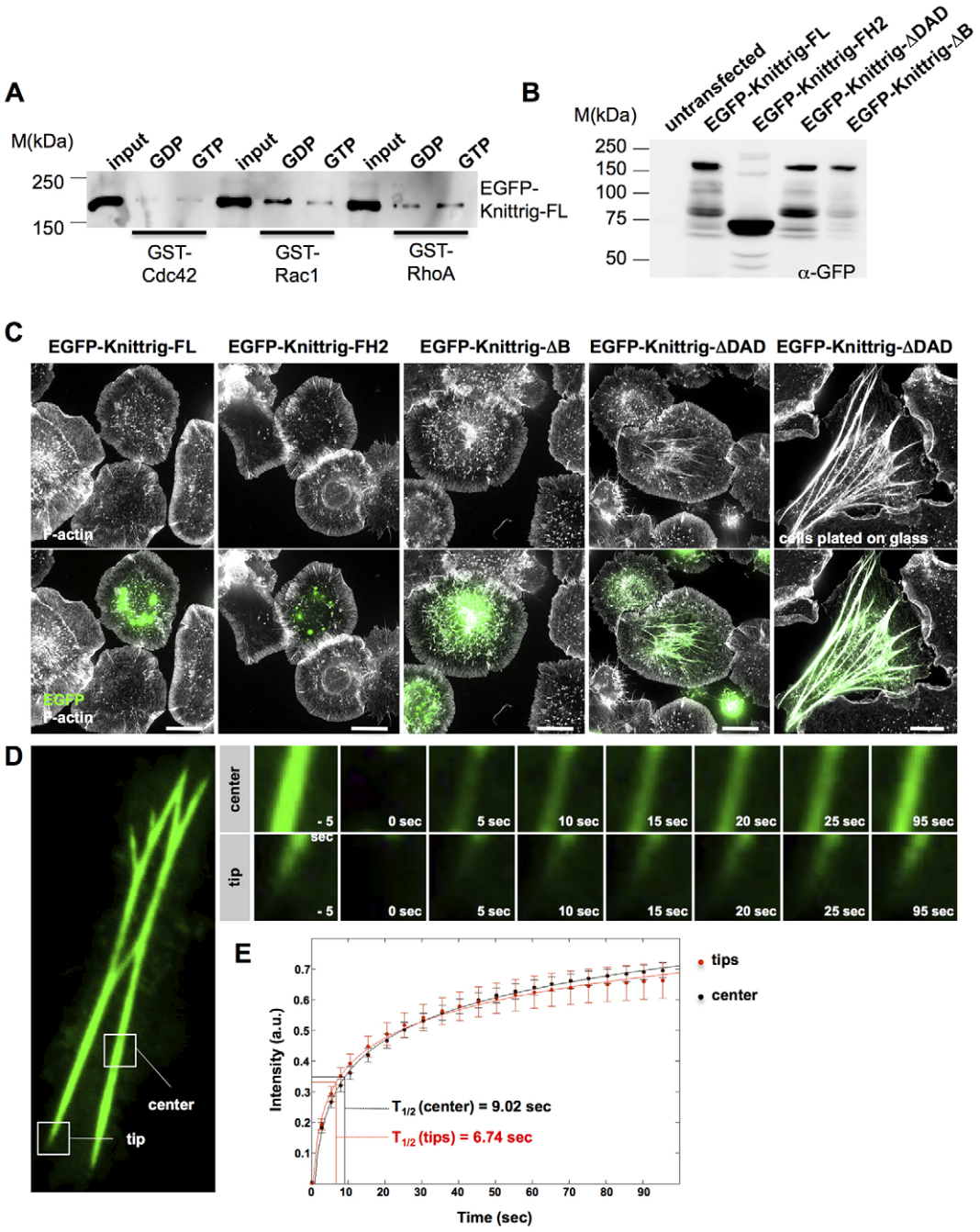

Fig. 6. Deletion of the C-terminal DAD activates Knittrig protein. (A) Pulldown experiments with GST-Rac1, GST-Rho1 and GST-Cdc42. GSH-sepharose-bound GST proteins were preloaded with GDP or GTPγS and incubated with lysate of S2R+ cells transfected with EGFP-Knittrig. Bead-bound complexes were probed for the presence of EGFP-Knittrig protein. (B) Western blot analysis of lysates of S2R+ cells transfected with the indicated EGFP-Knittrig constructs. (C) SIM image of S2R+ cells transfected with the indicated EGFP-Knittrig (green, EGFP) constructs and stained with phalloidin (white, F-actin). Cells were plated on ConA-treated coverslips, unless otherwise indicated. Scale bars: 10 µm. (D) Frames of spinning disc microscopy videos of an S2R+ cell expressing EGFP-Knittrig-ΔDAD (plated on glass) bleached subsequently at two separate positions (tip and center). (E) Fluorescence recovery curves of the two bleached regions. Data are means and s.e.m. of 13 (tip) and 25 (center) independent movies. Half-times of fluorescence recovery ($t_{1/2}$) were calculated from best linear fit (red and black curves).

ΔDAD results in a significant elevation in the level of F-actin (Fig. 8A). Similar to S2R+ cell transfection, the effect of Knittrig-ΔDAD expression on F-actin induction is more striking than that of Knittrig-ΔB (Fig. 8A). Interestingly, both truncated proteins also affect epithelial morphology. Epithelial cells overexpressing Knittrig-ΔDAD or Knittrig-ΔB in the *ptc* stripe constrict, resulting in apical invaginations.

We extended these gain-of-function studies to larval salivary glands. Gland cells are large polyploid cells that form a monolayered epithelial tube. In wild-type salivary gland cells, F-actin is mainly concentrated along the lateral cell boundaries, in the periluminal region and at the basal surface of gland cells (Fig. 8B). Expression of Knittrig-ΔDAD or Knittrig-ΔB dramatically reorganizes this irregularly shaped basal actin cytoskeleton to long

Development (2014) doi:10.1242/dev.101352

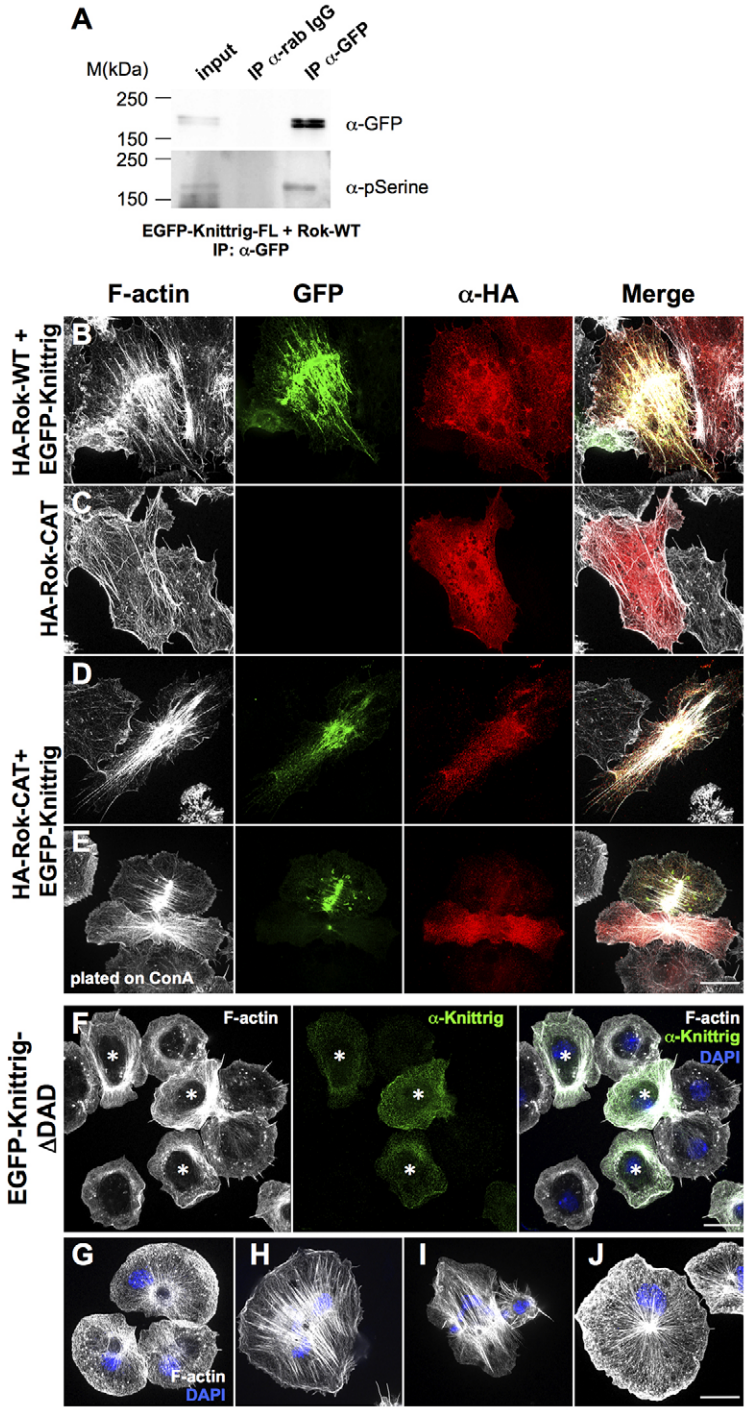

Fig. 7. Knittrig can be activated by Rok to induce stress fiber formation in S2 cells and macrophages. (A) Co-immunoprecipitation of full-length Knittrig from S2R+ cell lysate co-expressing EGFP-Knittrig and wild-type Rho kinase (Rok). Cell lysates were immunoprecipitated with a control preimmune serum or anti-GFP antibody. The immunoprecipitates were probed for the presence of EGFP and phosphoserine as indicated. (B-E) SIM images of S2R+ cells expressing (B) EGFP-Knittrig-FL and full-length HA-Rok-WT, (C) constitutively active HA-Rok-CAT (1-553aa) alone or (C) HA-Rok-CAT together with EGFP-Knittrig-FL, stained with phalloidin (white, F-actin), anti-HA (red, Rok) and EGFP (green, Knittrig). (F) SIM images of isolated macrophages expressing EGFP-Knittrig-ΔDAD, stained with phalloidin (white, F-actin), anti-Knittrig (red) and DAPI (blue, nuclei). Cells with elevated Knittrig-ΔDAD expression are marked by an asterisk. (G,H) SIM images of isolated macrophages expressing (G) full-length HA-Rok-WT, (H) EGFP-Knittrig-FL and HA-Rok-WT, (I) constitutively active HA-Rok-CA and (J) HA-Rok-CAT together with EGFP-Knittrig-FL. Cells are stained with phalloidin (white, F-actin) and DAPI (blue, nuclei). For expression in macrophages the combined Gal4/Gal80ts system was used. Heat shock was carried out in late third instar larvae at 29°C. Scale bars: 10 µm.

and thick actin bundles (Fig. 8B). This dramatic reorganization of the actin cytoskeleton also strongly affects overall gland morphology and multiple cyst-like lumina are found instead of the single lumen characteristic of wild-type glands (Fig. 8B). Interestingly, this multiple cyst phenotype has been observed recently upon expression of constitutively active Rho, again indicating that Knittrig may act downstream of Rho signaling (Xu et al., 2008).

These data clearly show that deletions of the autoinhibitory C-terminus result in activation of the Knittrig protein. Most importantly, our data demonstrate that constitutively active formins are able to induce actin stress fibers in *Drosophila*. We suggest that the function of Knittrig in trachea and macrophages depends on its ability to remodel the cell architecture by controlling the formation of unbranched F-actin bundles.

DISCUSSION

Formin proteins have been shown to regulate a variety of morphogenetic processes by controlling the structure and dynamics of the actin cytoskeleton both in individual cells and in tissue. *Drosophila knittrig* encodes a well-conserved FHOD formin protein. Here we focused on cell spreading and cell migration defects displayed by *knittrig* mutant macrophages, which relate to a disrupted actin cytoskeleton.

Development (2014) doi:10.1242/dev.101352

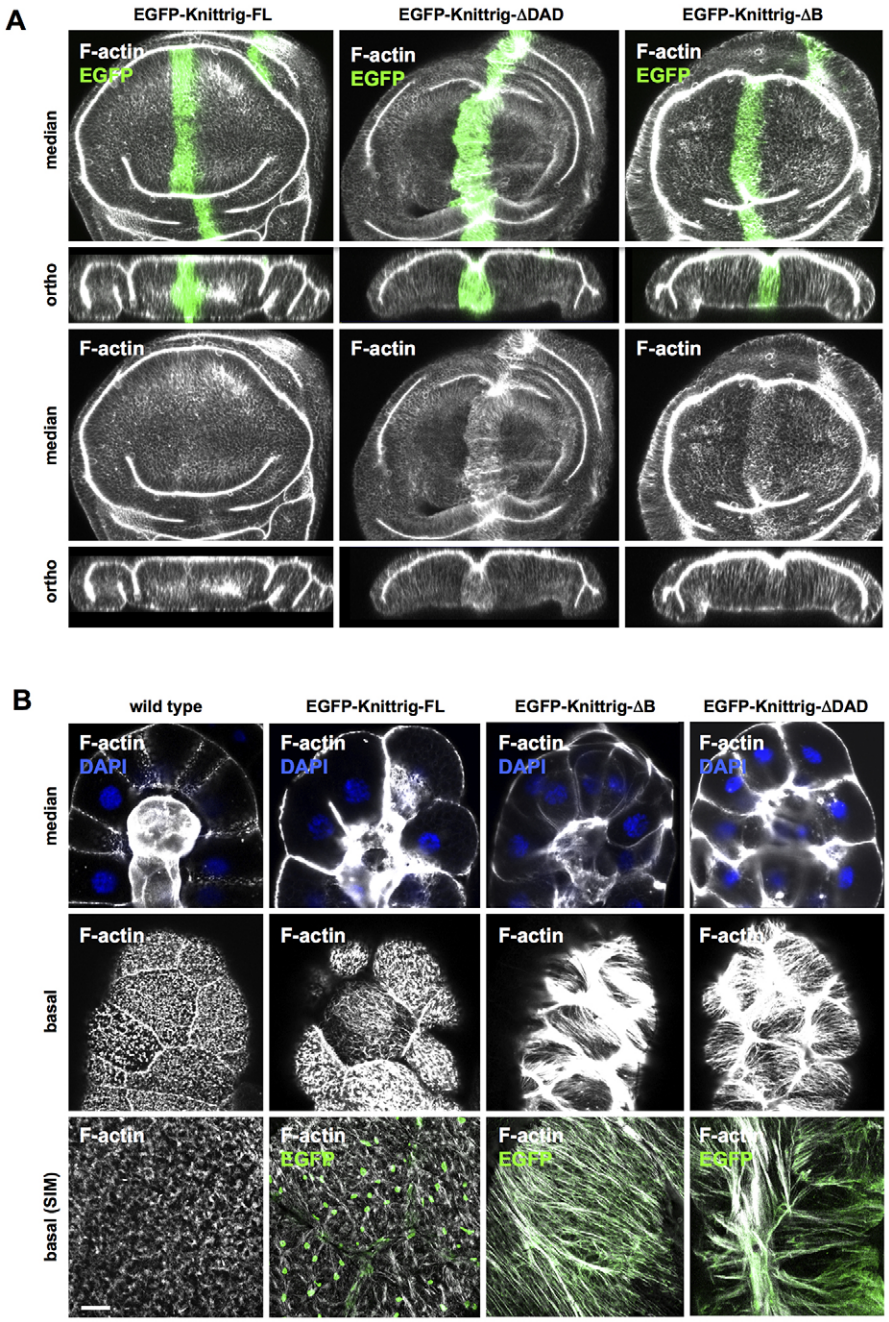

Fig. 8. Knittrig promotes stress fiber formation in *Drosophila*. (A) Single confocal sections of third instar larval wing imaginal discs stained for the indicated EGFP-Knittrig transgenes (green) and F-actin (phalloidin, white). Expression of full-length Knittrig (EGFP-Knittrig-FL) does not promote F-actin assembly in the *patched* stripe of the third instar wing disc. By contrast, expression of active EGFP-Knittrig-ΔDAD and EGFP-Knittrig-ΔB stimulates F-actin formation. (B) Single confocal sections of third instar larval salivary glands (distal region) stained for the indicated EGFP-Knittrig transgenes (green) and F-actin (phalloidin, white). SIM analysis shows a strong induction in actin stress fibers at the basal cell cortex of gland cells expressing Knittrig-ΔDAD or Knittrig-ΔB. Scale bar: 10 µm.

The molecular activities of formins on actin have been analyzed extensively. Formins are able to efficiently assemble linear actin filaments from profilin-bound actin monomers (Goode and Eck, 2007). The FH2 dimer nucleates filament assembly by stabilizing actin intermediates, whereas an additional processive capping activity of formins is thought to promote actin filament elongation by protecting growing barbed ends from capping proteins. Nucleation and processive elongation seem to be the major conserved activities of formins, although a number of studies also revealed additional effects on filament bundling, severing or even depolymerization (Harris et al., 2004; Harris et al., 2006; Schönichen et al., 2013). The broad range of biochemical activities suggest that formins regulate different aspects of the actin cytoskeleton architecture and actin dynamics during morphogenesis.

The phenotypic analyses of the formin mutants demonstrated distinct cellular functions in *Drosophila* development. The founding member of formins, Dia, is the key regulator of mitotic and meiotic cytokinesis in both the germline and all somatic cells, whereas the only member of the FMN formin subclass Capu is essential for anterior-posterior and dorsal-ventral patterning during oogenesis and early embryogenesis (Castrillon and Wasserman, 1994; Emmons et al., 1995; Manseau and Schüpbach, 1989). *form3* and *daam* mutants are embryonic/larval lethal owing to severe defects in tracheal development (Matusek et al., 2006; Tanaka et al., 2004).

Knittrig is also required for proper trachea development. Based on the distinct mutant phenotypes, all three formins seem to differentially regulate different aspects of tracheal morphogenesis. Tracheal tubes of *daam* mutant larvae fail to secrete the cuticle, whereas *form3* is required for tracheal cell fusion (Matusek et al.,

Development (2014) doi:10.1242/dev.101352

2006; Tanaka et al., 2004). The *knittrig* phenotype is much less dramatic and only affects the formation of distinct tracheal branches. Knittrig is not only expressed at tracheal tip cells but also strongly marks midline glial cells. However, we did not find significant defects in the morphology of *knittrig*-deficient glial cells (data not shown). This might suggest that Knittrig does not have a pronounced role in glia cell architecture. Alternatively, functional redundancy might exist between Knittrig and *CG32138*, which encodes a member of the FRL subclass of formins. *CG32138* has not been characterized but it is also expressed in CNS midline glia (Sánchez-Soriano et al., 2007).

Unlike other *Drosophila* formins, Knittrig is required for macrophage dynamics during the cellular wound response. Given its asymmetric enrichment at the rear of migrating macrophages we propose that Knittrig acts downstream of Rho/Rok-dependent cell protrusion. Like mammalian FHOD1, Knittrig binds GTPases such as Rho1 in a non-specific, nucleotide-independent manner. Thus, Knittrig seems not to be directly regulated by Rho1 but rather by the Rho effector kinase (Rok). In mammals, Rok in turn directly phosphorylates FHOD1 at three specific sites within the polybasic region of the DAD (Takeya et al., 2008). The phosphorylated serine/threonine residues are conserved in the Knittrig protein, which implies that its activity might also be regulated by phosphorylation in *Drosophila.* Serine phosphorylation is indeed enhanced upon Rok co-expression, indicating that Knittrig might be a direct substrate of Rok. Our gain-of-function experiments provide further evidence that Rok mediates the activation of Knittrig *in vivo*. Co-expression of Knittrig and Rok results in a strong induction of stress fibers. Consistently, we found that deletion of the polybasic region in Knittrig-ΔB promotes similar actin stress fiber formation. Thus, Rok-catalyzed phosphorylation is likely to disrupt an autoinhibitory interaction in Knittrig, as proposed recently for FHOD1 activation (Takeya et al., 2008).

Since the truncation of the complete DAD further increases the activity of Knittrig, additional regulatory mechanisms might be required for its full activation. Given the dramatic gain-of-function phenotype in flies, the cooperative functions of such regulatory signals might be essential to tightly restrict Knittrig activity during development. A possible regulatory scenario is simultaneous Rho1 binding and Rok-mediated phosphorylation, or even a phosphorylation-dependent increase in Rho1 binding. Alternative splicing would provide an additional regulatory mechanism to control formin function. The shortest isoform, Knittrig^{PB}, lacks the C-terminal DAD and hence constitutes a constitutively active protein. The expression of this active isoform seems to be upregulated in pupal salivary glands during ecdysone-induced programmed cell death (Anhezini et al., 2012). Thus, uncontrolled, massive induction of F-actin might be an efficient way to induce apoptosis or to extrude single cells from the epithelium, as proposed previously (Farhadifar et al., 2007).

It still remains unclear how formins, such as the FHOD proteins, induce actin stress fiber formation (Burridge and Wittchen, 2013). Based on sequence similarity, FHOD proteins have been grouped into the DRF class of formins likely to promote actin nucleation. Interestingly, the opposite has been observed recently *in vitro* (Schönichen and Geyer, 2010). In pyrene actin polymerization assays a recombinant FHOD1-ΔDAD behaves like an actin filament capping protein, inhibiting actin polymerization *in vitro*. High-speed sedimentation assays further showed that an N-terminal fragment lacking the FH2 domain is sufficient to bundle actin filaments. Based on these observations, the authors propose a model in which the dimeric FH2 domain protects barbed actin filament depolymerization, whereas the N-terminal region of FHOD bundles actin filaments. Thus, stress fiber formation might depend on the combination of actin capping and bundling activity rather than on actin nucleation and elongation (Schönichen and Geyer, 2010). However, recent studies on mouse Dia1 (Diap1) revealed that the DAD contains conserved residues essential for its nucleation activity (Gould et al., 2011). Thus, the nucleation activity of the truncated FHOD1-ΔDAD might have been lost and the remaining FH2 domain only stabilizes actin filaments. Interestingly, the critical residues for nucleation activity were mapped to a lysine followed by an arginine within the polybasic region, which is conserved in Knittrig as well as in mammalian FHOD1. *In vivo*, we found that constitutively active Knittrig is able to induce actin assembly. Expression of Knittrig-ΔDAD protein in the wing results in a significant increase of F-actin. However, it remains unclear whether increased F-actin is due to *de novo* actin nucleation or to stabilization of pre-existing actin filaments. Thus, in the future the activity of truncated proteins with an intact KR motif (the conserved lysine-arginine motif within the DAD) should be measured *in vitro*. Unfortunately, all our attempts to purify soluble full-length or truncated Knittrig proteins have proven unsuccessful so far.

In conclusion, the biological functions of Knittrig seem to be well conserved. Knittrig promotes stress fiber formation and macrophage migration. Re-expression of Knittrig not only rescues the migration defects of mutant cells but also increases the cellular immune response of macrophages. A similar positive activity of Knittrig in cell migration has recently been observed for human FHOD1, the expression of which is upregulated during epithelial-mesenchymal transition promoting cancer cell migration (Gardberg et al., 2013). Overexpression of human FHOD1 in melanoma and breast cancer cells promotes cell migration and cell invasion (Koka et al., 2003; Jurmeister et al., 2012). Likewise, recent *in vitro* data confirmed that FHOD1 is needed for directed forces and adhesion during cell spreading and migration (Iskratsch et al., 2013). Our data provide first insights into how FHOD proteins might promote cell migration *in vivo*. Given the asymmetric subcellular localization of Knittrig *in vivo* we propose that Knittrig promotes the formation of actin bundles at the rear of the cell in a Rok-dependent manner. Thus, Rok is in a central position to simultaneously coordinate actin assembly by Knittrig phosphorylation and the activation of actomyosin-based retraction by myosin light chain kinase (MLCK) phosphorylation in the trailing edge of migrating macrophages.

MATERIALS AND METHODS

Fly genetics

All crosses were performed at 25°C unless indicated otherwise. Excision mutagenesis was performed with the P(lwB)^{AA142} insertion as described (Stephan et al., 2011). The following deficiency chromosomes were used for mapping: *Df(3L)Scf-R6*, *Df(3L)hi22*, *Df(3L)BSC612*, *Df(3L)ED4421*, *Df(3L)ED4413* (obtained from the Bloomington Stock Center). To identify EMS-induced *knittrig* alleles we mutagenized isogenic *st e* marked chromosomes and screened in trans to *knittrig* excision alleles. Transgenic flies were generated using ΦC31-mediated transgenesis targeted to the *M{3xP3-RFP.attP}ZH-86F* landing site (Bischof et al., 2007). RNAi lines were obtained from the Vienna Drosophila RNAi Center (VDRC; ID 34034 and 34035). Flies bearing the pUASp-HA-Rok-WT and pUASp-HA-Rok-CAT (1-553aa) were obtained from Jennifer Zallen (Simões et al., 2010).

Cell culture, cell transfection and cloning

Drosophila S2R+ cells were propagated in 1× Schneider's *Drosophila* medium as described previously (Fricke et al., 2009). S2R+ cells were transfected as described previously (Fricke et al., 2009). A full-length Knittrig-PA cDNA construct was assembled using 5′ sequences of LD24110

to the first *Xho*I site and the remaining 3′ sequences from SD08909. cDNAs were amplified by PCR and subcloned into Gateway entry vectors (pENTR D-TOPO, Invitrogen) according to the manufacturer's instructions (*Escherichia coli* Expression System with Gateway Technology, Invitrogen). The QuikChange XL Site-Directed Mutagenesis Kit (Stratagene, Agilent Technologies) was used to generate distinct deletions. For primer details see supplementary material Table S1. The inserts were sequenced and cloned by LR *in vitro* recombination into corresponding destination vectors (Drosophila Genomics Resource Center) containing UASt promoters and N-terminal eGFP. The pQE-His-Tag system (Qiagen) was used to express fusion proteins used for immunization of rabbits. pUASp-HA-Rok-WT and pUASp-HA-Rok-CAT (1-553aa) plasmids were obtained from Jennifer Zallen (Simões et al., 2010).

Fluorescence recovery after photobleaching (FRAP) analysis

FRAP analysis of EGFP-Knittrig-ΔDAD was performed with an UltraVIEW Vox 3D live cell imaging system (PerkinElmer) coupled to a Nikon Eclipse Ti inverted microscope. The system incorporated a CSU-X1 spinning disk scanner (Yokogawa), a C9100-50 EM-CCD camera (1000×1000 pixels; (Hamamatsu) and Volocity software (PerkinElmer). Cells were imaged via a Nikon 60× (NA 1.49) oil-immersion objective lens. The fluorescence recovery was monitored by time-lapse imaging at low-intensity illumination and quantified with Volocity for FRAP (PerkinElmer).

Structured illumination microscopy (SIM) imaging

SIM images were taken with an ELYRA S.1 Microscope (CellObserver SD, 63×/1.4 oil-immersion objective; Zeiss) using software Zen 2010 D (Zeiss). Image acquisition was performed as described previously (Zobel and Bogdan, 2013). For isolation of macrophages, five white pupae or ten third instar larvae were bled into 400 µl Shields and Sang M3 medium containing 10% FBS and 1× penicillin/streptomycin. Cell suspensions were transferred to a chambered cover glass and cells were incubated for 1 hour at 25°C. Cell fixation and phalloidin staining were performed as previously described (Zobel and Bogdan, 2013).

In vivo migration assay of pupae

Live imaging of macrophages in prepupae and in the pupal wing was performed with a CellObserver SD spinning disk microscope (Zeiss) as reported (Sander et al., 2013). The cuticle of staged pupae [16 hours after puparium formation (APF)] were completely removed and pupae were placed on the lateral side, glued on glass-bottom culture plates. Cells were imaged through a 40× Plan-Apochromat (NA 1.3) oil-immersion objective using an inverted Zeiss Axio Observer.Z1 microscope with an Axiocam MRm CCD camera (6.45 µm × 6.45 µm) and 488 nm laser line. For wounding assays we used the UV laser ablation system DL-355/14 direct from Rapp OptoElectronics. ZEN software 2012 (Zeiss) was used for acquisition and processing of the images. For imaging living pupae or isolated macrophages we used the 488 nm argon laser at only 25% intensity to avoid photodamage.

Quantification of *in vivo* macrophage cell migration

To quantify the migration behavior we introduce the histogram-based macrophage migration score (HMMS). The score utilizes local histograms around the laser-induced wound to measure the macrophage concentration over time.

Let $I_1, ..., I_T$ be the images of a movie containing T frames (Fig. 5C). Since macrophages appear brighter than the background, thresholding can be used for cell segmentation. All pixels above a threshold k (manually selected for each movie) represent macrophages (Fig. 5D). Given the position $p=(x, y)$ of the laser-induced wound, concentric regions R_i (i=0, ..., 3) with an increasing radius $r_i=\rho+\rho i$ (where ρ is the mean radius of a single macrophage) are localized around p. Thus, R_0 describes a circular area covering the wound and R_1, R_2, R_3 are surrounding R_0 in the form of circular rings (i.e. annuli; Fig. 5E). All of the pixels that are not covered by regions $R_0, ..., R_3$ are described by region R_4. Since the wound is localized in the center of region R_0, this region should cover at least one macrophage after migration. Likewise, R_1 should cover several macrophages, since it surrounds R_0, as well as R_2 and R_3. All pixels that do not move towards the stimulus will remain in R_4.

Using this definition, migration towards the wound over time can now be interpreted as an increase in bright pixels in regions R_0-R_3, while the number of bright pixels decreases in R_4 (i.e. macrophages migrate from region R_4 over regions R_3, R_2 and R_1 towards region R_0; Fig. 5E). Given the threshold k, the macrophage occurrence for region i and frame t can be calculated by:

$$w(R_i,t)=\sum_{j=k+1}^{255} h_j^{R_i}(t)\,, \qquad (1)$$

where $h_j^{R_i}(t)$ is the normalized histogram value for intensity j in region R_i at time t. Again, if macrophages migrate towards the stimulus, $\omega(R_0, t)$, $\omega(R_1, t)$, $\omega(R_2, t)$ and $\omega(R_3, t)$ increase, while $\omega(R_4, t)$, decreases over time.

Given all macrophage occurrences for all regions over time, the HMMS is calculated by:

$$\mathrm{HMMS}(t)=\alpha_0\omega(R_0, t)+\alpha_1\omega(R_1, t)+\alpha_2\omega(R_2, t)+\alpha_3\omega(R_3, t)+\alpha_4\omega(R_4, t),$$

with weights α_0, α_1, α_2, α_3 >0 and α_4 <0. The weights α_0, α_1, α_2, α_3 are selected based on the two-dimensional Gaussian distribution $N(\mu, \Sigma)$, with mean value $\mu=p$ and covariance matrix:

$$\sum=\begin{pmatrix}\sigma^2 & 0\\ 0 & \sigma^2\end{pmatrix}, \qquad (2)$$

where α_0 is the volume (integral) covered by ± one standard deviation for each direction around the mean. Similarly, α_1 is the volume within (–2σ, +2σ) without the volume within (–σ, +σ). In the same manner, α_2 and α_3 are defined by the intervals (–3σ, +3σ) and (–4σ, +4σ), respectively. To punish macrophages remaining in region R_4, α_4 is set to –0.25. The HMMS will therefore increase over time, assuming that the macrophages migrate from region R_4 towards region R_0. To compare the migration behavior, HMMS values for several wild-type (n=11), *knittrig* RNAi (n=11) and *knittrig* mutant (n=15) movies were calculated. Finally, these values are normalized by $\mathrm{HMMS}(t)/\omega(U_{i=0}^{4}\ R_i,\ t)$, where the denominator is the percentage of foreground pixels relative to the total number of pixels. In this way, the score is adaptively restricted to cell migration only and independent of varying cell densities in different movies. Subsequently, median densities for all types were plotted (Fig. 5F).

GST pulldown and co-immunoprecipitation

An excess of recombinant GST-Rac1, GST-Cdc42 and GST-Rho1 (Grosshans et al., 2005) proteins was immobilized on glutathione resin according to the manufacturer's instructions (GE Healthcare). About 1×10^8 S2R+ cells were harvested and lysed in 2 ml ice-cold lysis buffer (1× PBS, 1% NP40, 1 mM DTT and 1 mM PMSF). Lysates were centrifuged for 10 minutes at 10,000 ***g*** (4°C) and 500 µl of the cytoplasmic supernatant were added to 30 µl loaded glutathione resin. Following incubation for 1 hour at room temperature, unbound proteins were removed by washing four times with 1 ml lysis buffer at room temperature. 10% of the preparation was used per lane on standard SDS-PAGE and analyzed by western blot. The immobilized GST proteins were pre-treated with either 1 mM GDP or 1 mM GTP-γS plus 25 mM $MgCl_2$ supplement for 10 minutes at 30°C. Co-immunoprecipitation experiments were performed as previously described (Fricke et al., 2009). Phosphorylated serine/threonine residues were detected using an anti-phosphoserine antibody (PSR-45, Abcam).

Acknowledgements

We thank J. Grosshans for sharing plasmids for expression of recombinant GST proteins; Jennifer Zallen for providing UASp-Rok plasmids and flies; Sandford I. Bernstein for providing *Prm*^{1} flies; Peter Hanley and Markus Horsthemke for help with FRAP analysis; S. Mackensen and M. van Cann for help during cloning, transgenesis and quantification; and the Bloomington Stock Center and VDRC for fly strains.

Competing interests

The authors declare no competing financial interests.

Author contributions

S.B. oversaw the biochemical, genetic and cell biological work. U.L. generated the *knittrig* mutant flies, performed the complementation analysis and *in situ*

hybridization experiments. M.B. characterized the *knittrig* mutant macrophages, performed the rescue and live-imaging experiments. B.R. and D.B. established the histogram-based image analysis. A.F. performed the S2 cell transfection and western blot analysis. I.B. sequenced the mutant alleles. X.J. oversaw the bioinformatic analyses. C.K. oversaw the initial fly genetics experiments. S.B. wrote the manuscript with assistance from all authors.

Funding

This work was supported by grants to S.B. and X.J. from the Cluster Of Excellence 'Cells in Motion' (CIM), and by grants to S.B. from the Heisenberg Program of the Deutsche Forschungsgemeinschaft (DFG).

Supplementary material

Supplementary material available online at
http://dev.biologists.org/lookup/suppl/doi:10.1242/dev.101352/-/DC1

References

Anhezini, L., Saita, A. P., Costa, M. S., Ramos, R. G. and Simon, C. R. (2012). Fhos encodes a Drosophila Formin-like protein participating in autophagic programmed cell death. *Genesis* **50**, 672-684.

Bischof, J., Maeda, R. K., Hediger, M., Karch, F. and Basler, K. (2007). An optimized transgenesis system for Drosophila using germ-line-specific phiC31 integrases. *Proc. Natl. Acad. Sci. USA* **104**, 3312-3317.

Bogdan, S. and Klämbt, C. (2003). Kette regulates actin dynamics and genetically interacts with Wave and Wasp. *Development* **130**, 4427-4437.

Burridge, K. and Wittchen, E. S. (2013). The tension mounts: stress fibers as force-generating mechanotransducers. *J. Cell Biol.* **200**, 9-19.

Campellone, K. G. and Welch, M. D. (2010). A nucleator arms race: cellular control of actin assembly. *Nat. Rev. Mol. Cell Biol.* **11**, 237-251.

Carlier, M. F., Husson, C., Renault, L. and Didry, D. (2011). Control of actin assembly by the WH2 domains and their multifunctional tandem repeats in Spire and Cordon-Bleu. *Int. Rev. Cell Mol. Biol.* **290**, 55-85.

Castrillon, D. H. and Wasserman, S. A. (1994). Diaphanous is required for cytokinesis in Drosophila and shares domains of similarity with the products of the limb deformity gene. *Development* **120**, 3367-3377.

Chevrier, V., Piel, M., Collomb, N., Saoudi, Y., Frank, R., Paintrand, M., Narumiya, S., Bornens, M. and Job, D. (2002). The Rho-associated protein kinase p160ROCK is required for centrosome positioning. *J. Cell Biol.* **157**, 807-817.

Emmons, S., Phan, H., Calley, J., Chen, W., James, B. and Manseau, L. (1995). Cappuccino, a Drosophila maternal effect gene required for polarity of the egg and embryo, is related to the vertebrate limb deformity locus. *Genes Dev.* **9**, 2482-2494.

Englund, C., Uv, A. E., Cantera, R., Mathies, L. D., Krasnow, M. A. and Samakovlis, C. (1999). adrift, a novel bnl-induced Drosophila gene, required for tracheal pathfinding into the CNS. *Development* **126**, 1505-1514.

Farhadifar, R., Röper, J. C., Aigouy, B., Eaton, S. and Jülicher, F. (2007). The influence of cell mechanics, cell-cell interactions, and proliferation on epithelial packing. *Curr. Biol.* **17**, 2095-2104.

Firat-Karalar, E. N. and Welch, M. D. (2011). New mechanisms and functions of actin nucleation. *Curr. Opin. Cell Biol.* **23**, 4-13.

Fricke, R., Gohl, C., Dharmalingam, E., Grevelhörster, A., Zahedi, B., Harden, N., Kessels, M., Qualmann, B. and Bogdan, S. (2009). Drosophila Cip4/Toca-1 integrates membrane trafficking and actin dynamics through WASP and SCAR/WAVE. *Curr. Biol.* **19**, 1429-1437.

Gardberg, M., Kaipio, K., Lehtinen, L., Mikkonen, P., Heuser, V. D., Talvinen, K., Iljin, K., Kampf, C., Uhlen, M., Grénman, R. et al. (2013). FHOD1, a formin upregulated in epithelial-mesenchymal transition, participates in cancer cell migration and invasion. *PLoS ONE* **8**:e74923.

Gasteier, J. E., Madrid, R., Krautkrämer, E., Schröder, S., Muranyi, W., Benichou, S. and Fackler, O. T. (2003). Activation of the Rac-binding partner FHOD1 induces actin stress fibers via a ROCK-dependent mechanism. *J. Biol. Chem.* **278**, 38902-38912.

Gasteier, J. E., Schroeder, S., Muranyi, W., Madrid, R., Benichou, S. and Fackler, O. T. (2005). FHOD1 coordinates actin filament and microtubule alignment to mediate cell elongation. *Exp. Cell Res.* **306**, 192-202.

Goode, B. L. and Eck, M. J. (2007). Mechanism and function of formins in the control of actin assembly. *Annu. Rev. Biochem.* **76**, 593-627.

Gould, C. J., Maiti, S., Michelot, A., Graziano, B. R., Blanchoin, L. and Goode, B. L. (2011). The formin DAD domain plays dual roles in autoinhibition and actin nucleation. *Curr. Biol.* **21**, 384-390.

Grosshans, J., Wenzl, C., Herz, H. M., Bartoszewski, S., Schnorrer, F., Vogt, N., Schwarz, H. and Müller, H. A. (2005). RhoGEF2 and the formin Dia control the formation of the furrow canal by directed actin assembly during Drosophila cellularisation. *Development* **132**, 1009-1020.

Harris, E. S., Li, F. and Higgs, H. N. (2004). The mouse formin, FRLalpha, slows actin filament barbed end elongation, competes with capping protein, accelerates polymerization from monomers, and severs filaments. *J. Biol. Chem.* **279**, 20076-20087.

Harris, E. S., Rouiller, I., Hanein, D. and Higgs, H. N. (2006). Mechanistic differences in actin bundling activity of two mammalian formins, FRL1 and mDia2. *J. Biol. Chem.* **281**, 14383-14392.

Hotulainen, P. and Lappalainen, P. (2006). Stress fibers are generated by two distinct actin assembly mechanisms in motile cells. *J. Cell Biol.* **173**, 383-394.

Iskratsch, T., Lange, S., Dwyer, J., Kho, A. L., dos Remedios, C. and Ehler, E. (2010). Formin follows function: a muscle-specific isoform of FHOD3 is regulated by CK2 phosphorylation and promotes myofibril maintenance. *J. Cell Biol.* **191**, 1159-1172.

Iskratsch, T., Yu, C. H., Mathur, A., Liu, S., Stévenin, V., Dwyer, J., Hone, J., Ehler, E. and Sheetz, M. (2013). FHOD1 Is Needed for Directed Forces and Adhesion Maturation during Cell Spreading and Migration. *Dev. Cell* **27**, 545-559.

Jani, K. and Schöck, F. (2007). Zasp is required for the assembly of functional integrin adhesion sites. *J. Cell Biol.* **179**, 1583-1597.

Johansson, K. C., Metzendorf, C. and Söderhäll, K. (2005). Microarray analysis of immune challenged Drosophila hemocytes. *Exp. Cell Res.* **305**, 145-155.

Jurmeister, S., Baumann, M., Balwierz, A., Keklikoglou, I., Ward, A., Uhlmann, S., Zhang, J. D., Wiemann, S. and Sahin, Ö. (2012). MicroRNA-200c represses migration and invasion of breast cancer cells by targeting actin-regulatory proteins FHOD1 and PPM1F. *Mol. Cell. Biol.* **32**, 633-651.

Kadandale, P., Stender, J. D., Glass, C. K. and Kiger, A. A. (2010). Conserved role for autophagy in Rho1-mediated cortical remodeling and blood cell recruitment. *Proc. Natl. Acad. Sci. USA* **107**, 10502-10507.

Kan-O, M., Takeya, R., Abe, T., Kitajima, N., Nishida, M., Tominaga, R., Kurose, H. and Sumimoto, H. (2012a). Mammalian formin Fhod3 plays an essential role in cardiogenesis by organizing myofibrillogenesis. *Biol. Open* **1**, 889-896.

Kan-O, M., Takeya, R., Taniguchi, K., Tanoue, Y., Tominaga, R. and Sumimoto, H. (2012b). Expression and subcellular localization of mammalian formin Fhod3 in the embryonic and adult heart. *PLoS ONE* **7**, e34765.

Klämbt, C., Jacobs, J. R. and Goodman, C. S. (1991). The midline of the Drosophila central nervous system: a model for the genetic analysis of cell fate, cell migration, and growth cone guidance. *Cell* **64**, 801-815.

Koka, S., Neudauer, C. L., Li, X., Lewis, R. E., McCarthy, J. B. and Westendorf, J. J. (2003). The formin-homology-domain-containing protein FHOD1 enhances cell migration. *J. Cell Sci.* **116**, 1745-1755.

Kovar, D. R. (2006). Molecular details of formin-mediated actin assembly. *Curr. Opin. Cell Biol.* **18**, 11-17.

Kunda, P., Craig, G., Dominguez, V. and Baum, B. (2003). Abi, Sra1, and Kette control the stability and localization of SCAR/WAVE to regulate the formation of actin-based protrusions. *Curr. Biol.* **13**, 1867-1875.

Leung, T., Chen, X. Q., Manser, E. and Lim, L. (1996). The p160 RhoA-binding kinase ROK alpha is a member of a kinase family and is involved in the reorganization of the cytoskeleton. *Mol. Cell. Biol.* **16**, 5313-5327.

Liu, H., Mardahl-Dumesnil, M., Sweeney, S. T., O'Kane, C. J. and Bernstein, S. I. (2003). Drosophila paramyosin is important for myoblast fusion and essential for myofibril formation. *J. Cell Biol.* **160**, 899-908.

Liu, R., Linardopoulou, E. V., Osborn, G. E. and Parkhurst, S. M. (2010). Formins in development: orchestrating body plan origami. *Biochim. Biophys. Acta* **1803**, 207-225.

Manseau, L. J. and Schüpbach, T. (1989). cappuccino and spire: two unique maternal-effect loci required for both the anteroposterior and dorsoventral patterns of the Drosophila embryo. *Genes Dev.* **3**, 1437-1452.

Matusek, T., Djiane, A., Jankovics, F., Brunner, D., Mlodzik, M. and Mihály, J. (2006). The Drosophila formin DAAM regulates the tracheal cuticle pattern through organizing the actin cytoskeleton. *Development* **133**, 957-966.

McGuire, S. E., Le, P. T., Osborn, A. J., Matsumoto, K. and Davis, R. L. (2003). Spatiotemporal rescue of memory dysfunction in Drosophila. *Science* **302**, 1765-1768.

Mi-Mi, L., Votra, S., Kemphues, K., Bretscher, A. and Pruyne, D. (2012). Z-line formins promote contractile lattice growth and maintenance in striated muscles of C. elegans. *J. Cell Biol.* **198**, 87-102.

Moreira, C. G., Jacinto, A. and Prag, S. (2013). Drosophila integrin adhesion complexes are essential for hemocyte migration in vivo. *Biol. Open* **2**, 795-801.

Otomo, T., Tomchick, D. R., Otomo, C., Panchal, S. C., Machius, M. and Rosen, M. K. (2005). Structural basis of actin filament nucleation and processive capping by a formin homology 2 domain. *Nature* **433**, 488-494.

Pollard, T. D. and Borisy, G. G. (2003). Cellular motility driven by assembly and disassembly of actin filaments. *Cell* **112**, 453-465.

Pollard, T. D. and Cooper, J. A. (2009). Actin, a central player in cell shape and movement. *Science* **326**, 1208-1212.

Sánchez-Madrid, F. and Serrador, J. M. (2009). Bringing up the rear: defining the roles of the uropod. *Nat. Rev. Mol. Cell Biol.* **10**, 353-359.

Sánchez-Soriano, N., Tear, G., Whitington, P. and Prokop, A. (2007). Drosophila as a genetic and cellular model for studies on axonal growth. *Neural Dev.* **2**, 9.

Sander, M., Squarr, A. J., Risse, B., Jiang, X. and Bogdan, S. (2013). Drosophila pupal macrophages – a versatile tool for combined ex vivo and in vivo imaging of actin dynamics at high resolution. *Eur. J. Cell Biol.* **92**, 349-354.

Schönichen, A. and Geyer, M. (2010). Fifteen formins for an actin filament: a molecular view on the regulation of human formins. *Biochim. Biophys. Acta* **1803**, 152-163.

Schönichen, A., Mannherz, H. G., Behrmann, E., Mazur, A. J., Kühn, S., Silván, U., Schoenenberger, C. A., Fackler, O. T., Raunser, S., Dehmelt, L. et al. (2013). FHOD1 is a combined actin filament capping and bundling factor that selectively associates with actin arcs and stress fibers. *J. Cell Sci.* **126**, 1891-1901.

Schulte, A., Stolp, B., Schönichen, A., Pylypenko, O., Rak, A., Fackler, O. T. and Geyer, M. (2008). The human formin FHOD1 contains a bipartite structure of FH3 and GTPase-binding domains required for activation. *Structure* **16**, 1313-1323.

Simões, S. M., Blankenship, J. T., Weitz, O., Farrell, D. L., Tamada, M., Fernandez-Gonzalez, R. and Zallen, J. A. (2010). Rho-kinase directs Bazooka/Par-3 planar polarity during Drosophila axis elongation. *Dev. Cell* **19**, 377-388.

Sinenko, S. A. and Mathey-Prevot, B. (2004). Increased expression of Drosophila tetraspanin, Tsp68C, suppresses the abnormal proliferation of ytr-deficient and Ras/Raf-activated hemocytes. *Oncogene* **23**, 9120-9128.
Stephan, R., Gohl, C., Fleige, A., Klämbt, C. and Bogdan, S. (2011). Membrane-targeted WAVE mediates photoreceptor axon targeting in the absence of the WAVE complex in Drosophila. *Mol. Biol. Cell* **22**, 4079-4092.
Takeya, R. and Sumimoto, H. (2003). Fhos, a mammalian formin, directly binds to F-actin via a region N-terminal to the FH1 domain and forms a homotypic complex via the FH2 domain to promote actin fiber formation. *J. Cell Sci.* **116**, 4567-4575.
Takeya, R., Taniguchi, K., Narumiya, S. and Sumimoto, H. (2008). The mammalian formin FHOD1 is activated through phosphorylation by ROCK and mediates thrombin-induced stress fibre formation in endothelial cells. *EMBO J.* **27**, 618-628.
Tanaka, H., Takasu, E., Aigaki, T., Kato, K., Hayashi, S. and Nose, A. (2004). Formin3 is required for assembly of the F-actin structure that mediates tracheal fusion in Drosophila. *Dev. Biol.* **274**, 413-425.
Taniguchi, K., Takeya, R., Suetsugu, S., Kan-O, M., Narusawa, M., Shiose, A., Tominaga, R. and Sumimoto, H. (2009). Mammalian formin fhod3 regulates actin assembly and sarcomere organization in striated muscles. *J. Biol. Chem.* **284**, 29873-29881.
Thompson, J. D., Higgins, D. G. and Gibson, T. J. (1994). CLUSTAL W: improving the sensitivity of progressive multiple sequence alignment through sequence weighting, position-specific gap penalties and weight matrix choice. *Nucleic Acids Res.* **22**, 4673-4680.
Valanne, S., Kleino, A., Myllymäki, H., Vuoristo, J. and Rämet, M. (2007). Iap2 is required for a sustained response in the Drosophila Imd pathway. *Dev. Comp. Immunol.* **31**, 991-1001.
Westendorf, J. J. (2001). The formin/diaphanous-related protein, FHOS, interacts with Rac1 and activates transcription from the serum response element. *J. Biol. Chem.* **276**, 46453-46459.
Westendorf, J. J. and Koka, S. (2004). Identification of FHOD1-binding proteins and mechanisms of FHOD1-regulated actin dynamics. *J. Cell. Biochem.* **92**, 29-41.
Wood, W. and Jacinto, A. (2007). Drosophila melanogaster embryonic haemocytes: masters of multitasking. *Nat. Rev. Mol. Cell Biol.* **8**, 542-551.
Xu, N., Keung, B. and Myat, M. M. (2008). Rho GTPase controls invagination and cohesive migration of the Drosophila salivary gland through Crumbs and Rho-kinase. *Dev. Biol.* **321**, 88-100.
Zobel, T. and Bogdan, S. (2013). A high resolution view of the fly actin cytoskeleton lacking a functional WAVE complex. *J. Microsc.* **251**, 224-231.

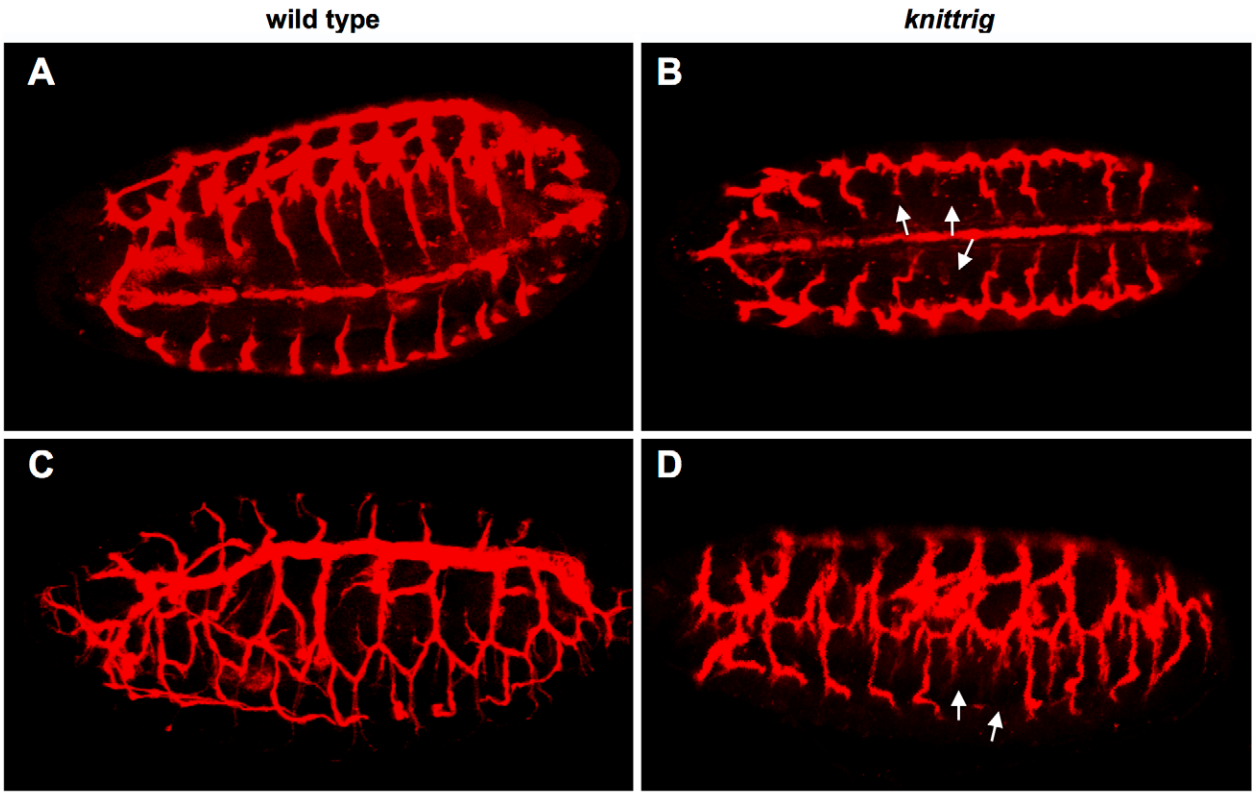

Fig. S1. *knittrig* function is required in trachea cells. Defects in the embryonic tracheal-system in *knittrig* mutant embryos are shown. To visualize the tracheae tau-lacZ transgene was driven under control of the *btl*-gal4 in mutant embryos. In the mutant embryos one or more ganglionic branches are not formed properly (arrows in B, D) in comparison to wild type embryos (A, C).

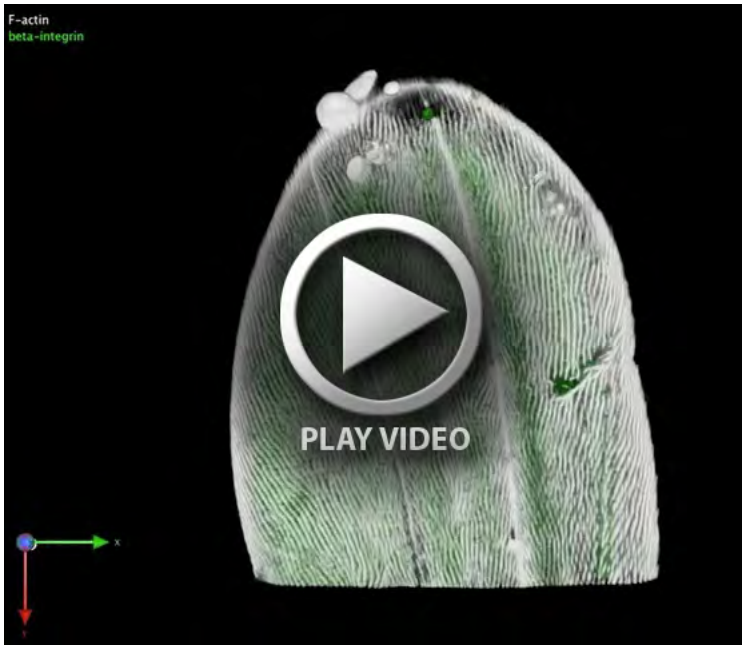

Movie 1. 3D reconstruction of a *knittrig* mutant wing of a late pupa (36h APF), reconstructed from confocal images, co-stained for F-actin (phalloidin, white) and β-integrin (green). No morphological defects are visible.

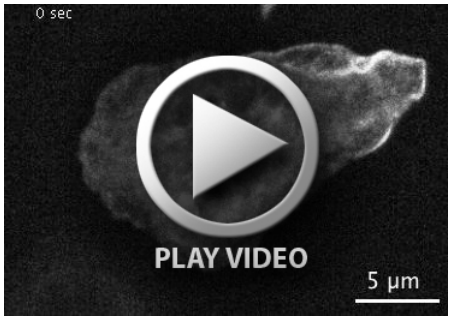

Movie 2. Spinning disc microscopy video of an isolated pupal macrophage expressing EGFP-tagged full-length Knittrig driven by the *hml*Δ-gal4 driver, immediately recorded after plating.

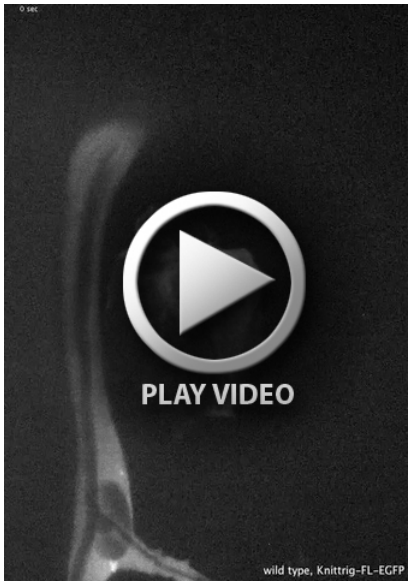

Movie 3. Random migration of a macrophage expressing EGFP-Knittrig-FL imaged from a wild type pupa (4 APF). The cell migrates along a trachea.

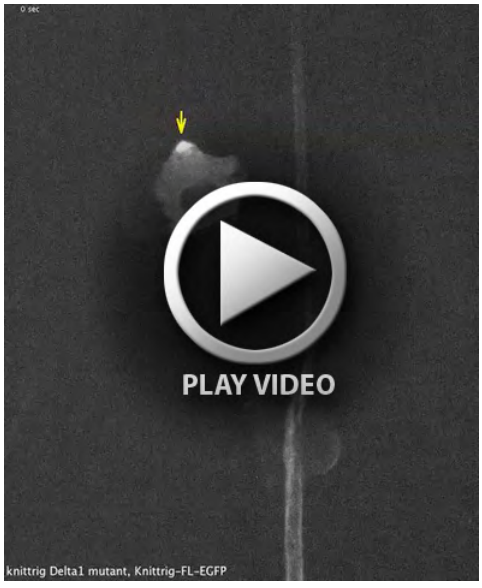

Movie 4. (a,b) Two examples of macrophages expressing EGFP-Knittrig-FL imaged from a *knittrig*$^{\Delta 1}$ mutant pupa (4 APF). The positions of the dynamic Knittrig localization is marked by yellow arrows.

Movie 5. Directed cell migration of wild type macrophages expressing cytoplasmic EGFP imaged from a wing of a wild type pupa (20 APF) upon laser induced ablation of a single cell (position is marked by yellow circle).

Movie 6. Directed cell migration of *knittrig*$^{\Delta 1}$ mutant macrophages imaged from a pupal wing (20 APF) upon laser induced ablation of a single cell.

Movie 7. Directed cell migration of rescued *knittrig*$^{\Delta 1}$ mutant macrophages imaged from a pupal wing (20 APF) upon laser induced ablation of a single cell.

Movie 8.

Movie 9.

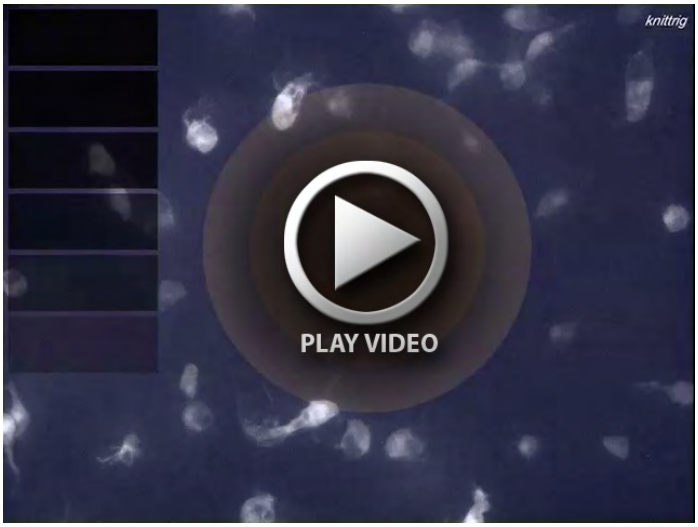

Movie 10.

Movie 11.

Movies 8-11. Exemplary movies are given for wild type (M8), *knittrig* RNAi (M9), *knittrig*$^{\Delta 1}$ (M10) and rescued *knittrig*$^{\Delta 1}$ macrophages (M11). Calculated macrophage occurrences $\omega(R_i, t)$ are given for region R_0, R_1, R_2, R_3 and R_4 in red, dark orange, bright orange, yellow and blue respectively. The purple plot illustrates the *HMMS*(t). Note that the y-axes scaling is adjusted during calculation. The values in the plots for regions R_0-R_4 increase the more macrophages are located in these regions. The *HMMS*(t) increases with dense macrophage concentrations in R_0-R_3 and decreases with dense concentrations in R_4.

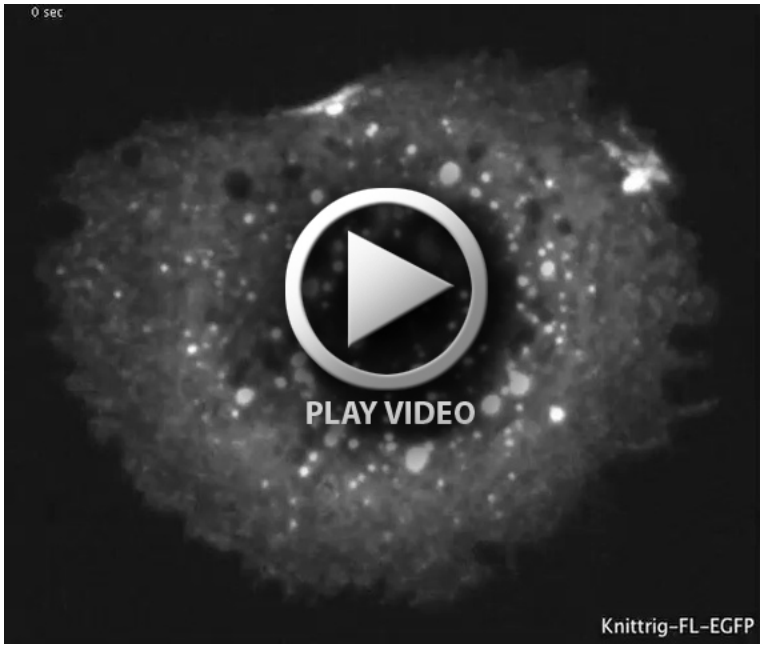

Movie 12. Video of a S2R+ cells expressing EGFP-Knittrig-FL, plated on glass.

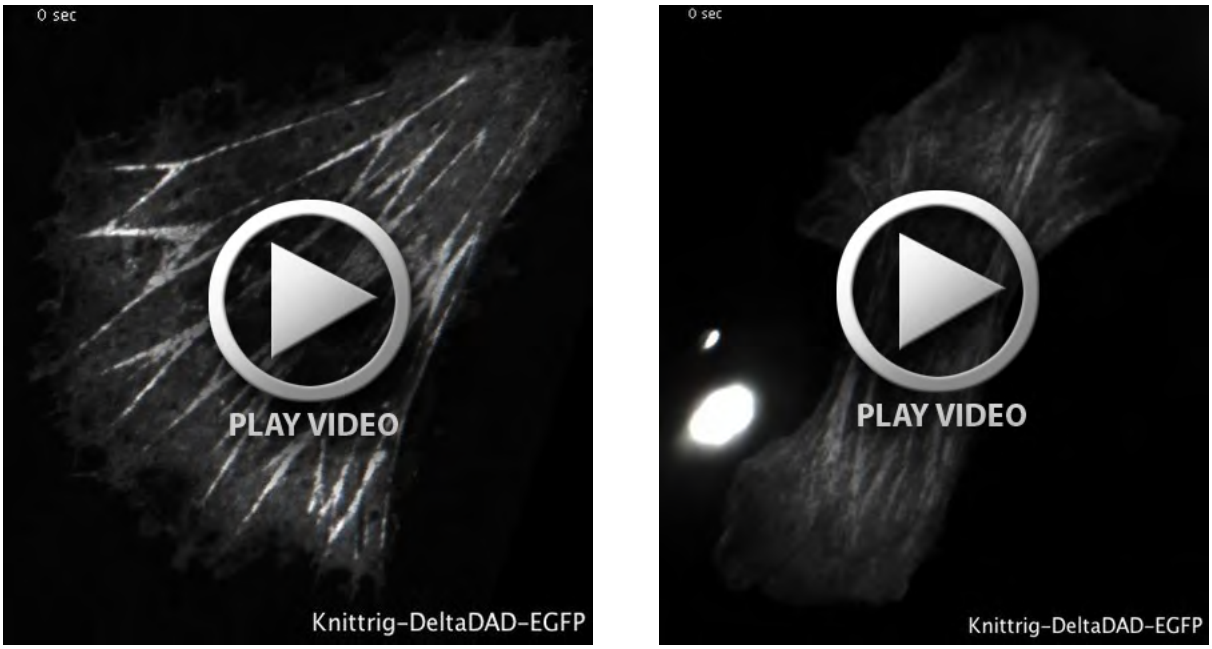

Movie 13. (a,b) Two videos of S2R+ cells expressing EGFP-Knittrig-ΔDAD, plated on glass.

Movie 14. Video of a S2R+ cell expressing EGFP-Knittrig-ΔDAD, bleached at indicated regions at the tip and in the center of Knittrig marked stress fibers.

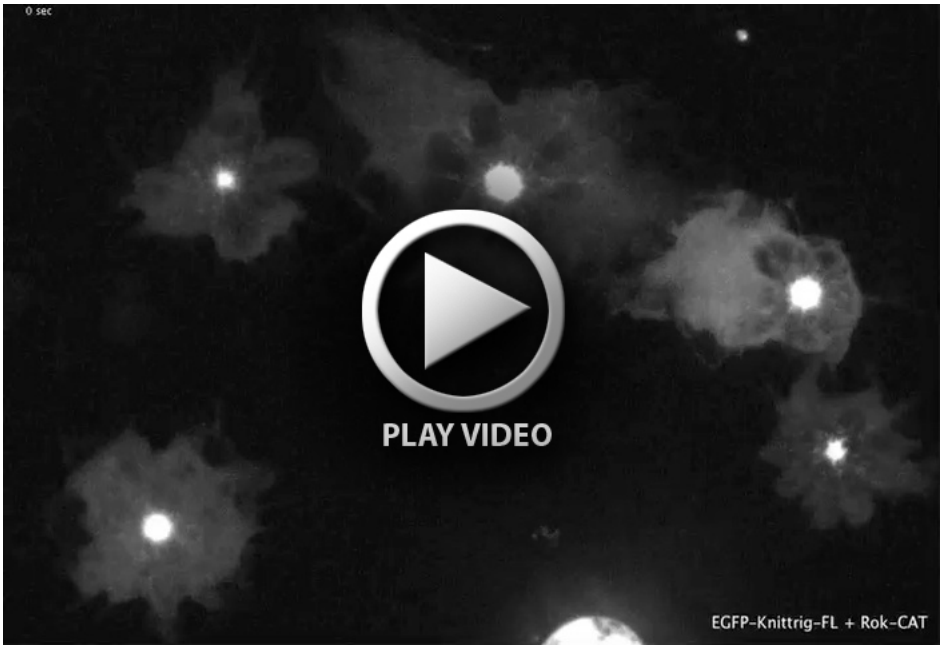

Movie 15. Video of S2R+ cells expressing EGFP-Knittrig-FL (white) together with activated Rho kinase Rok-CAT.

Movie 16. Video of S2R+ cells expressing EGFP-Knittrig-FL (white) together with activated Rho kinase Rok-CAT and Tubulin-Cherry (red).

Table S1. Primers

Primer name	Sequence	Destination vector
5-Knittrig-PA-FL-TOPO	CACCATGATTGTGAAAATGGAGCCGG	pENTR/pUASt-attB-rfa-EGFP
3-Knittrig-PA-FL-TOPO	CTAATAGGTTTGTATCAAGGCAGCC	pENTR/pUASt-attB-rfa-EGFP
3-Knittrig-PA-ΔDAD-TOPO	CTAGTCGCCATCGGTGAACTGC	pENTR/pUASt-attB-rfa-EGFP
3-Knittrig-PA-ΔB-TOPO	CTACGGCGTTGTCCGTGTTCCTG	pENTR/pUASt-attB-rfa-EGFP
5-Knittrig-PA-FH2-TOPO	CACCATGAGCTTGGCACCACCACCCATG	pENTR/pUASt-attB-rfa-EGFP
3-Knittrig-PA-FH2-TOPO	CTAGAACTGCTCCTCGCTTTGGC	pENTR/pUASt-attB-rfa-EGFP